Quantum Monte Carlo simulations of ultracold fermions on optical lattices within dynamical mean-field theory

Nils Blümer and Elena Gorelik, Univ. Mainz

Outline

Systems with strong electronic/fermionic correlations

Paramagnetic Mott metal-insulator transition

Prototype example: V_2O_3 doped
with Cr/Ti and/or under pressure

Phase diagram

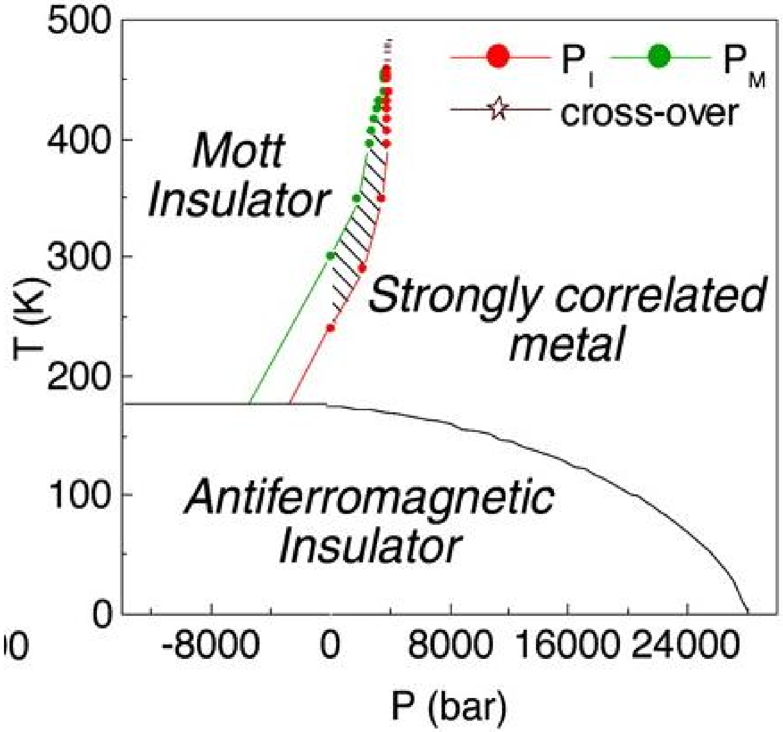

Systems with strong electronic/fermionic correlations

Paramagnetic Mott metal-insulator transition

Prototype example: V_2O_3 doped with Cr/Ti and/or under pressure

Phase diagram

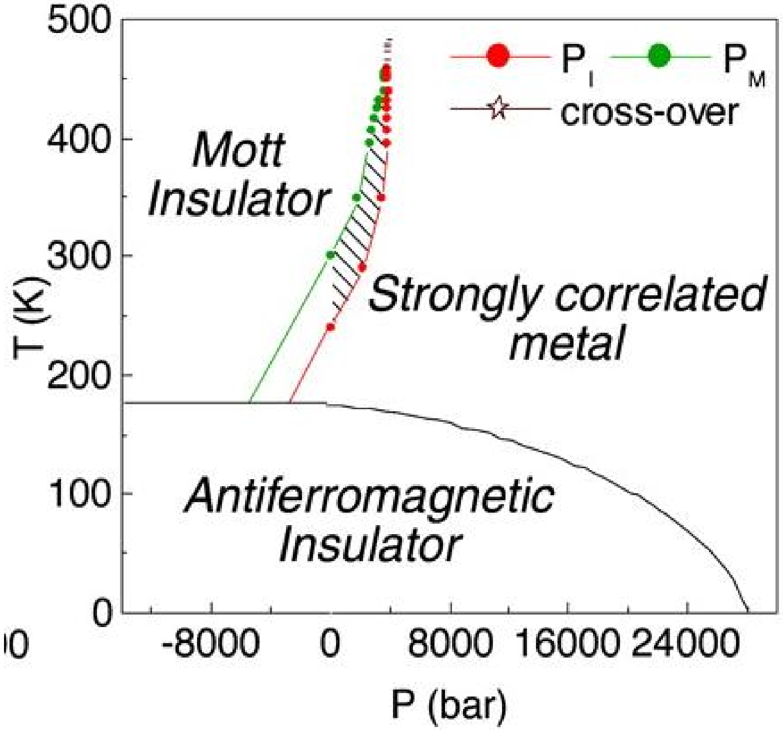

Electrical conductivity

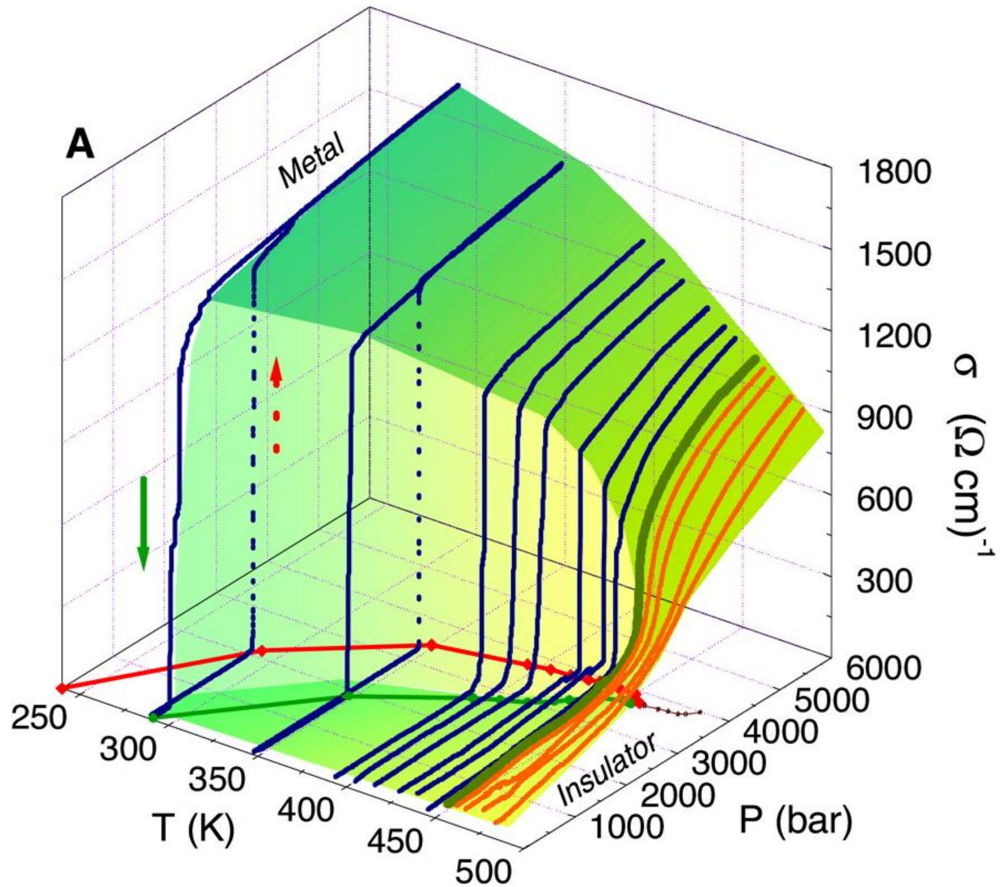

[Limelette et al., Science 302, 89 (2003)]

Complex phases of cuprate and organic superconductors

High-T_c physics contained in 2D Hubbard model?

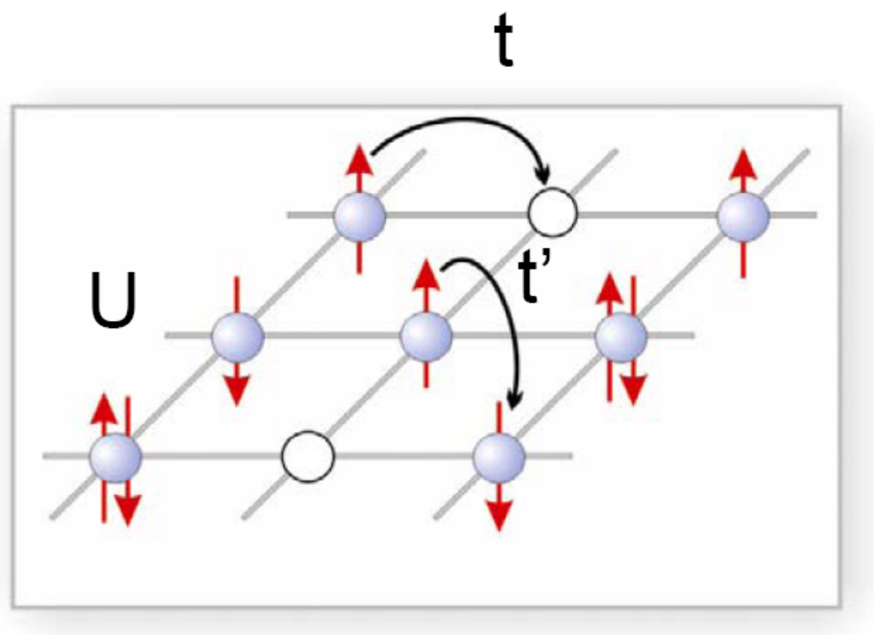

Are antiferromagnetic (AF) and Mott insulating phases essential for superconductivity?

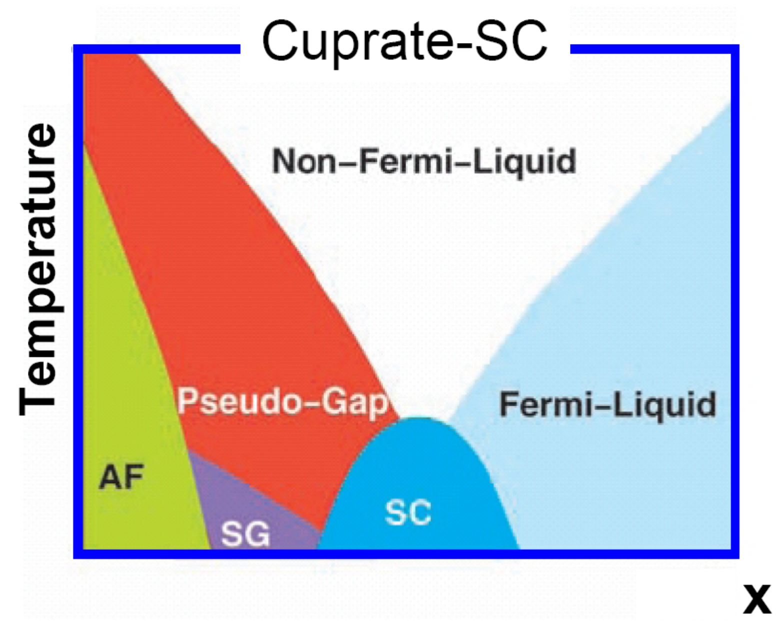

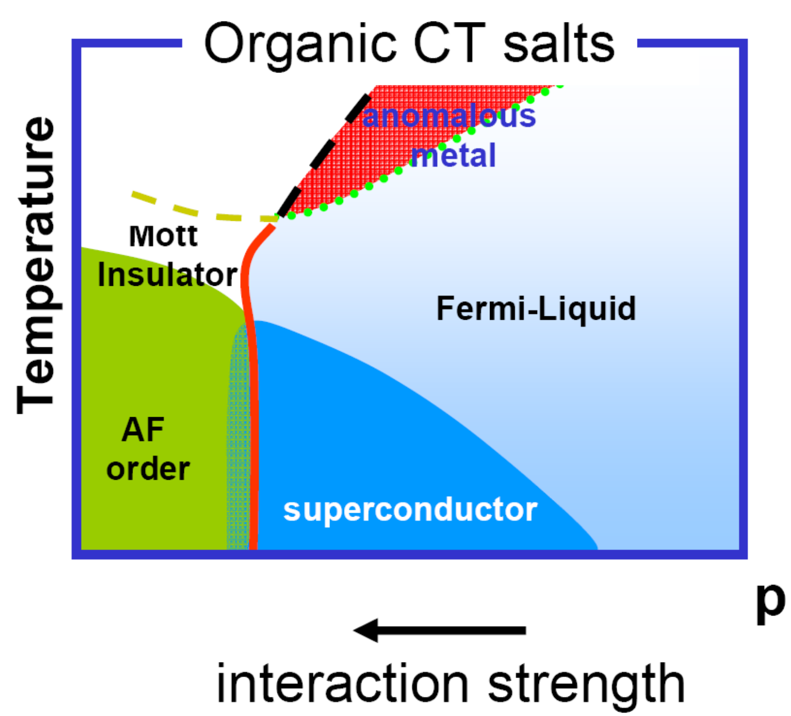

Correlated ultracold quantum gases on optical lattices: basics

Experimental systems: small dilute clouds of about 10^6 ultracold atoms $\rightsquigarrow$ need trap

Optical dipole trap (2 beams)

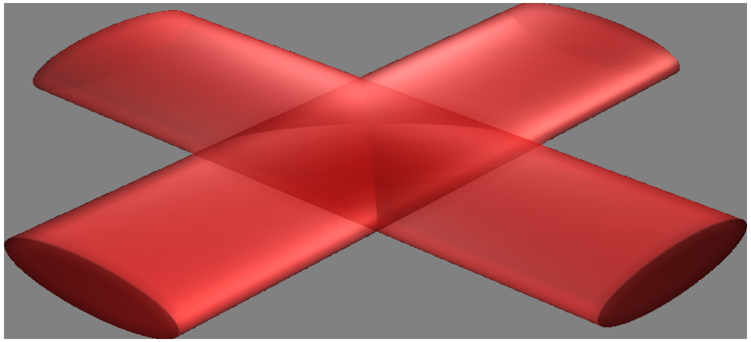

$$V_{\text{dipole}}(\boldsymbol{r}) = -\boldsymbol{d} \cdot \boldsymbol{E}(\boldsymbol{r}) \propto \alpha(\omega_{\text{L}}) \, |\boldsymbol{E}(\boldsymbol{r})|^2$$

time-averaged
intensity $|\boldsymbol{E}(\boldsymbol{r})|^2$

Correlated ultracold quantum gases on optical lattices: basics

Experimental systems: small dilute clouds of about 10^6 ultracold atoms $\rightsquigarrow$ need trap

Optical dipole trap (2 beams)

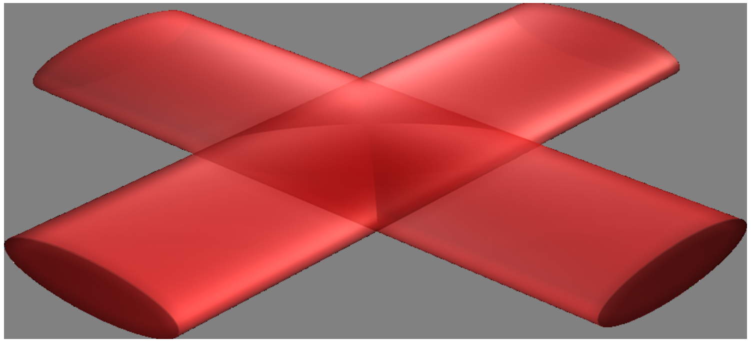

$$V_{\text{dipole}}(\boldsymbol{r}) = -\boldsymbol{d} \cdot \boldsymbol{E}(\boldsymbol{r}) \propto \alpha(\omega_L)\,|\boldsymbol{E}(\boldsymbol{r})|^2$$

time-averaged intensity $|\boldsymbol{E}(\boldsymbol{r})|^2$

polarizability $\alpha(\omega_L)$ changes sign at ω_0

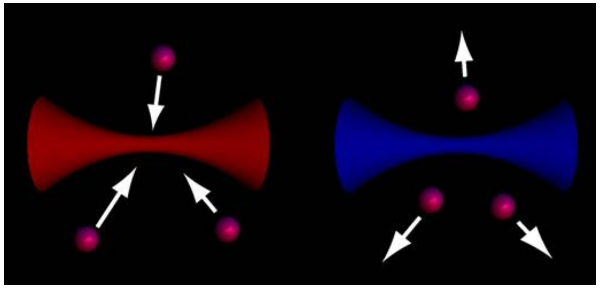

Correlated ultracold quantum gases on optical lattices: basics

Experimental systems: small dilute clouds of about 10^6 ultracold atoms $\rightsquigarrow$ need trap

Optical dipole trap (2 beams)

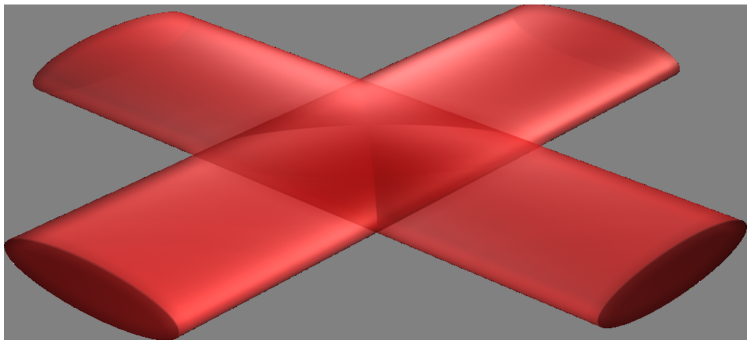

$$V_{\text{dipole}}(\boldsymbol{r}) = -\boldsymbol{d} \cdot \boldsymbol{E}(\boldsymbol{r}) \propto \alpha(\omega_{\text{L}}) \, |\boldsymbol{E}(\boldsymbol{r})|^2$$

time-averaged intensity $|\boldsymbol{E}(\boldsymbol{r})|^2$

polarizability $\alpha(\omega_{\text{L}})$ changes sign at ω_0

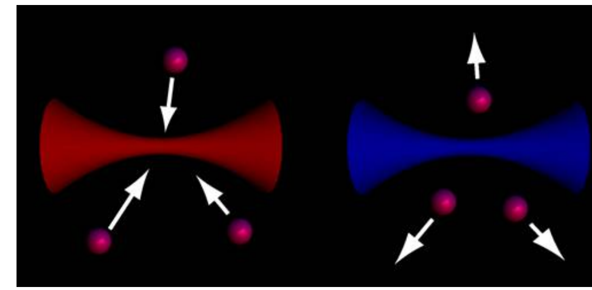

Standing wave (from coherent counterpropagating beams) $\rightsquigarrow$ modulated potential

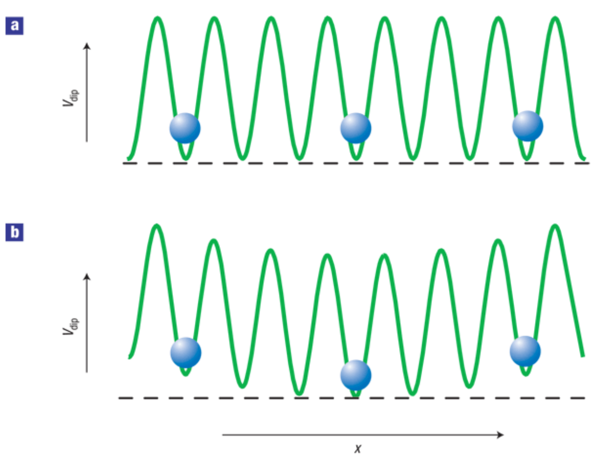

Beam profile: (anti) trapping

Correlated ultracold quantum gases on optical lattices: basics

Experimental systems: small dilute clouds of about 10^6 ultracold atoms $\rightsquigarrow$ need trap

Optical dipole trap (2 beams)

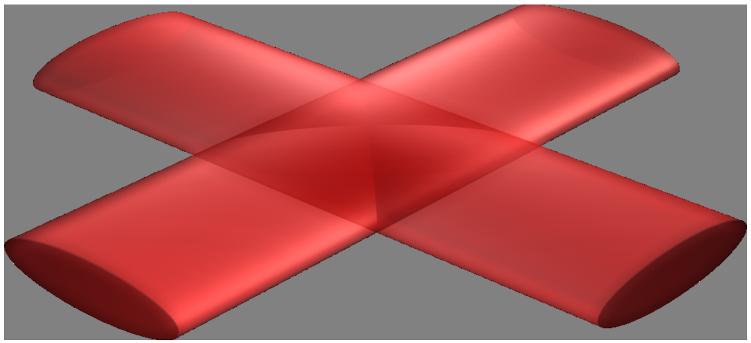

$$V_{\text{dipole}}(\boldsymbol{r}) = -\boldsymbol{d} \cdot \boldsymbol{E}(\boldsymbol{r}) \propto \alpha(\omega_{\text{L}})\,|\boldsymbol{E}(\boldsymbol{r})|^2$$

time-averaged intensity $|\boldsymbol{E}(\boldsymbol{r})|^2$

polarizability $\alpha(\omega_{\text{L}})$ changes sign at ω_0

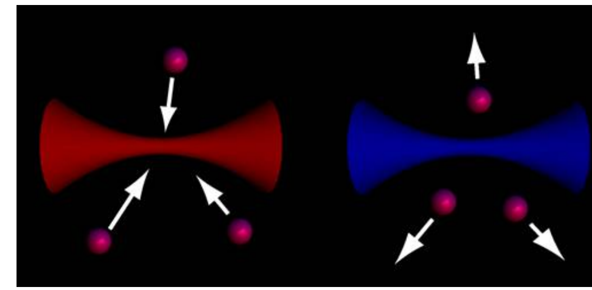

Standing wave (from coherent counterpropagating beams) $\rightsquigarrow$ modulated potential

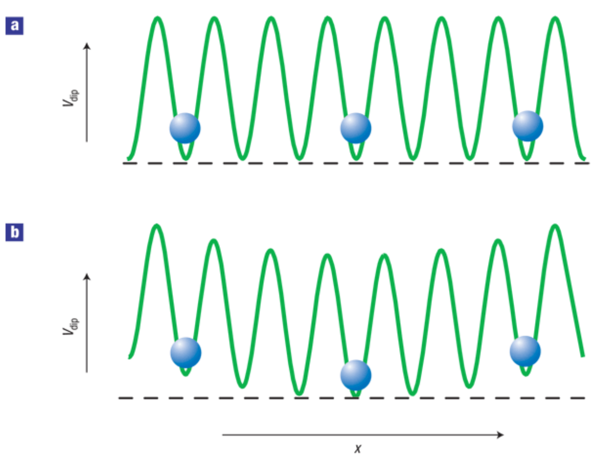

Beam profile: (anti) trapping

1 pair of lasers $\rightsquigarrow$ pancakes

2 pairs of lasers $\rightsquigarrow$ tubes

3 pairs of lasers $\rightsquigarrow$ 3D lattice

hopping t tunable by laser

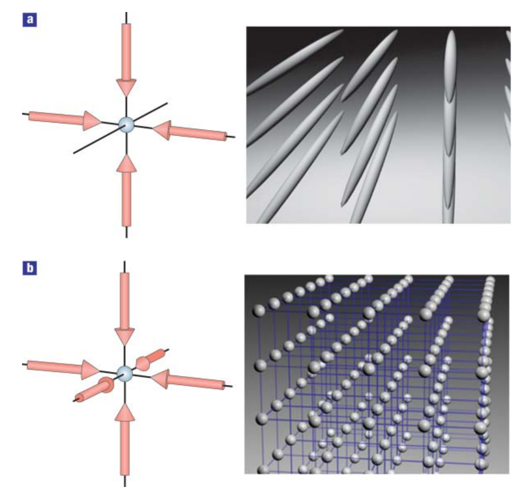

Interactions can be tuned via Feshbach resonances

Interactions can be tuned via Feshbach resonances (here in magnetic field $\boldsymbol{B}$)

short ranged: characterized by scattering length a – both signs possible!

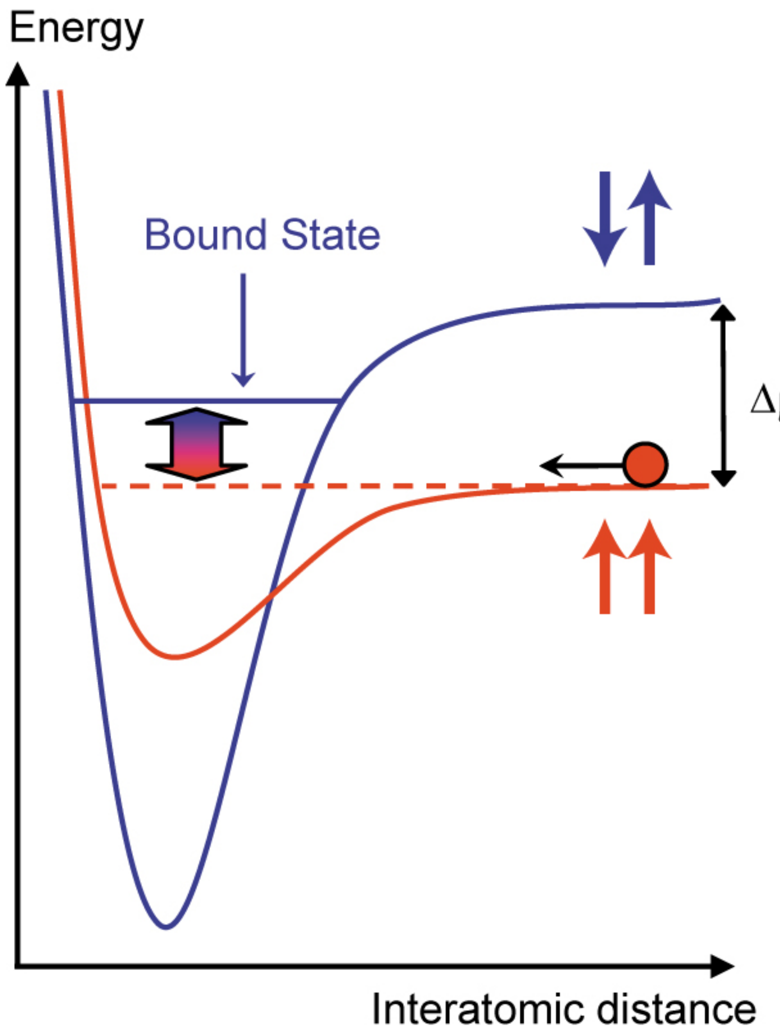

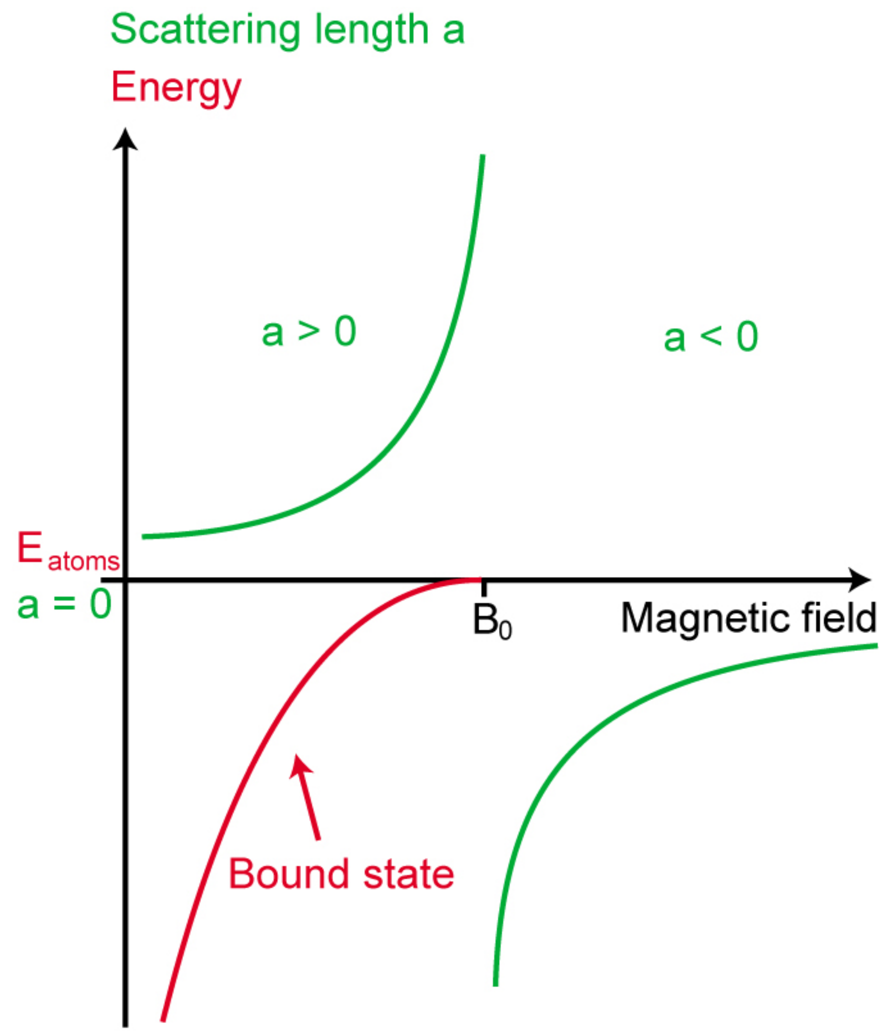

Correlated ultracold quantum gases on optical lattices: bosons

First evidence of strongly correlations in cold atoms: bosonic Mott transition

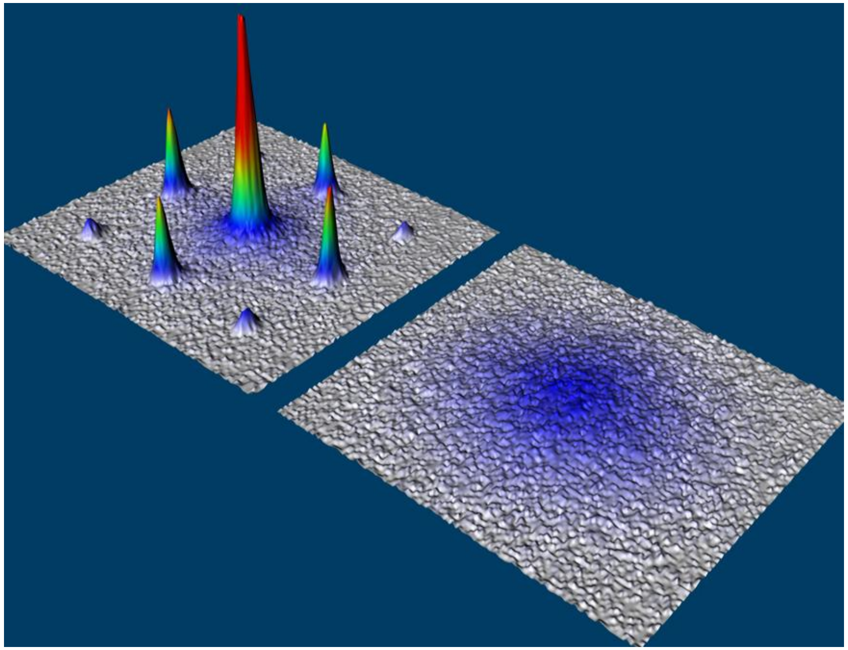

ultracold bosons on optical lattice (Bloch group, 2002)

Time-of-flight image – momentum distribution

Correlated ultracold quantum gases on optical lattices: bosons

First evidence of strongly correlations in cold atoms: bosonic Mott transition

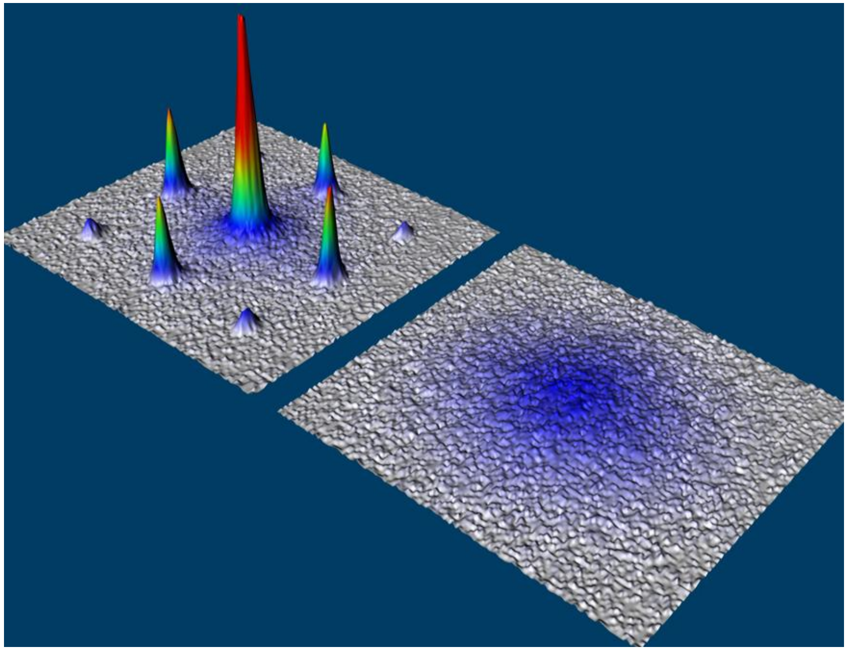

ultracold bosons on optical lattice (Bloch group, 2002)

Time-of-flight image – momentum distribution

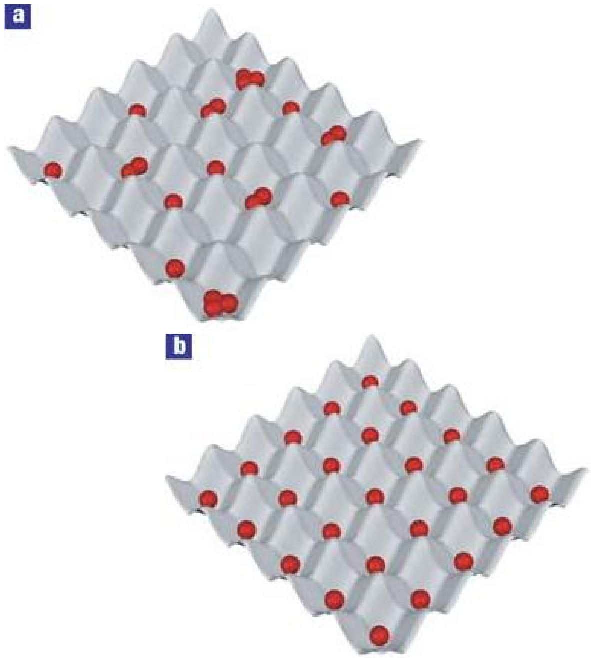

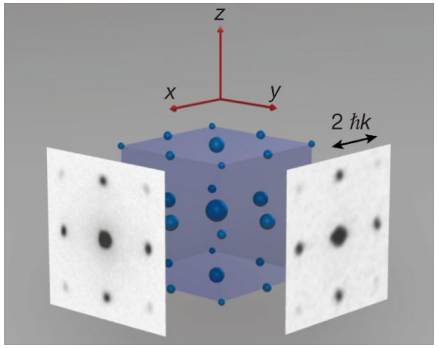

Correlated ultracold quantum gases on optical lattices: bosons

First evidence of strongly correlations in cold atoms: bosonic Mott transition

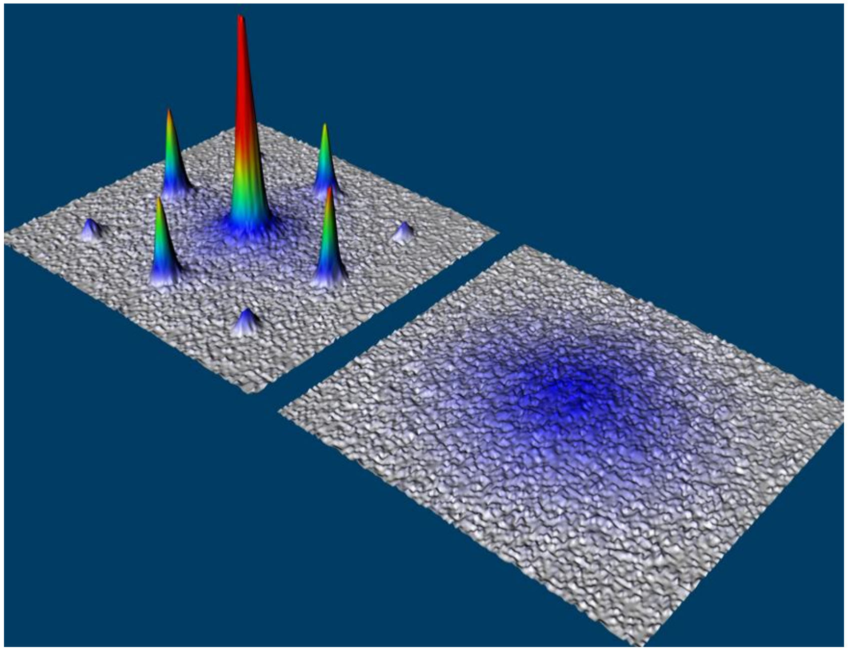

Time-of-flight image – momentum distribution

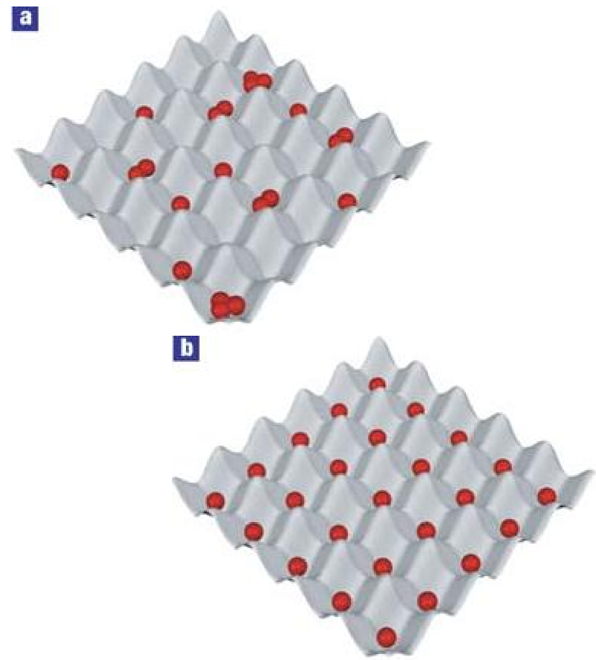

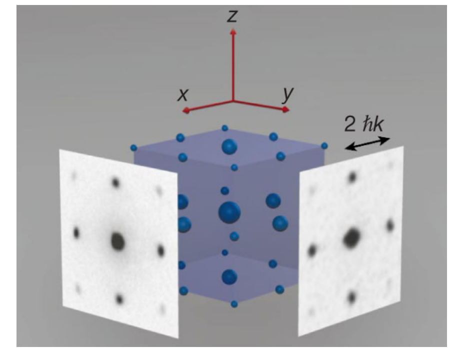

ultracold bosons on optical lattice (Bloch group, 2002)

superfluidity destroyed by density constraint at large U;
trapping potential $\rightsquigarrow$ wedding cake structure

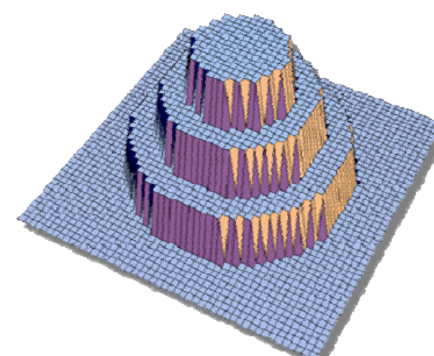

Correlated ultracold quantum gases on optical lattices: fermions

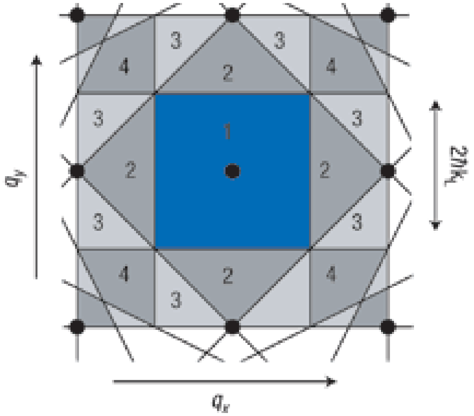

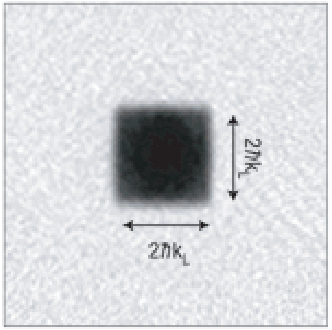

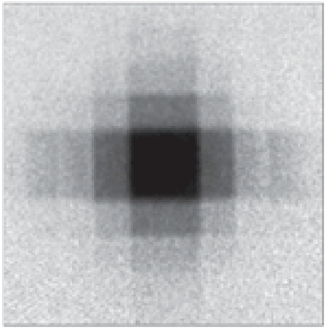

1 species: band insulator for filled 1st Brillouin zone:

[Köhl et al, PRL (2005)]

Correlated ultracold quantum gases on optical lattices: fermions

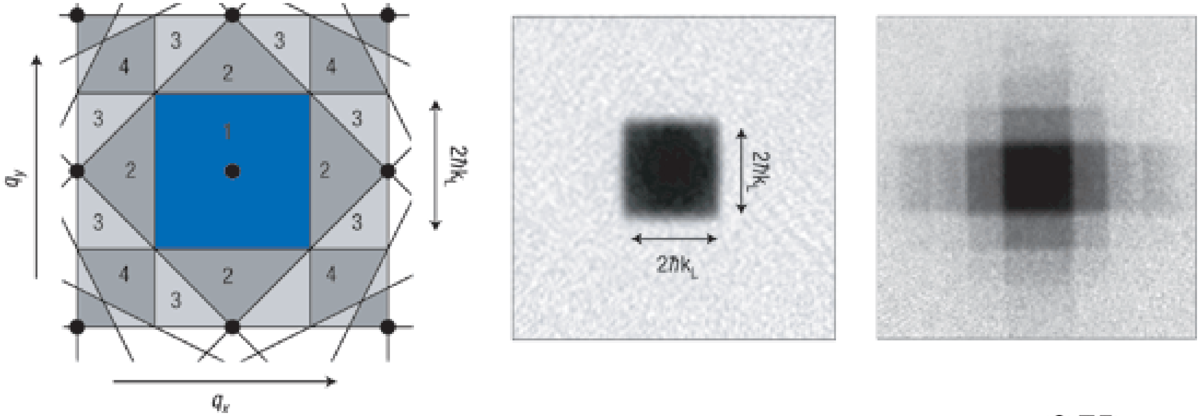

1 species: band insulator for filled 1st Brillouin zone:

[Köhl et al, PRL (2005)]

Recent breakthrough: paramagnetic Mott transition in 2-flavor mixtures

Detection method: measure cloud diameter vs. trap strength

Simulations (here DMFT+NRG) essential for interpretation of data!

[Schneider et al, Science **322**, 1520 (2008)]

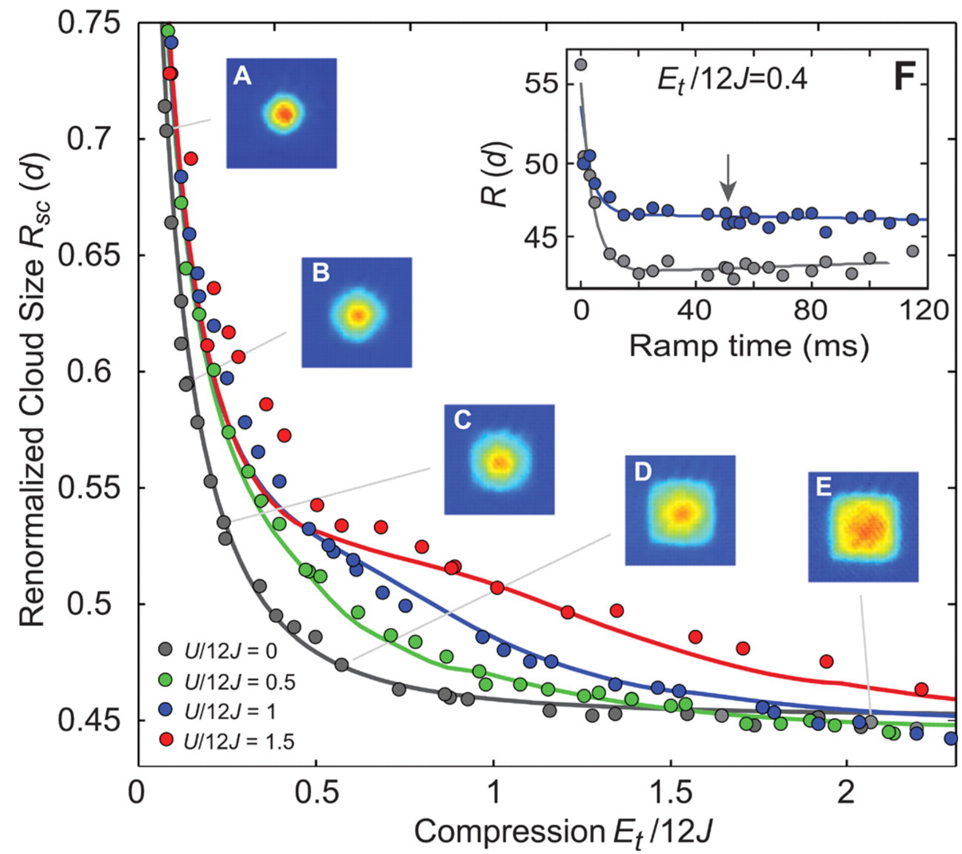

Further MIT observables: column density, fraction of atoms with double occupations

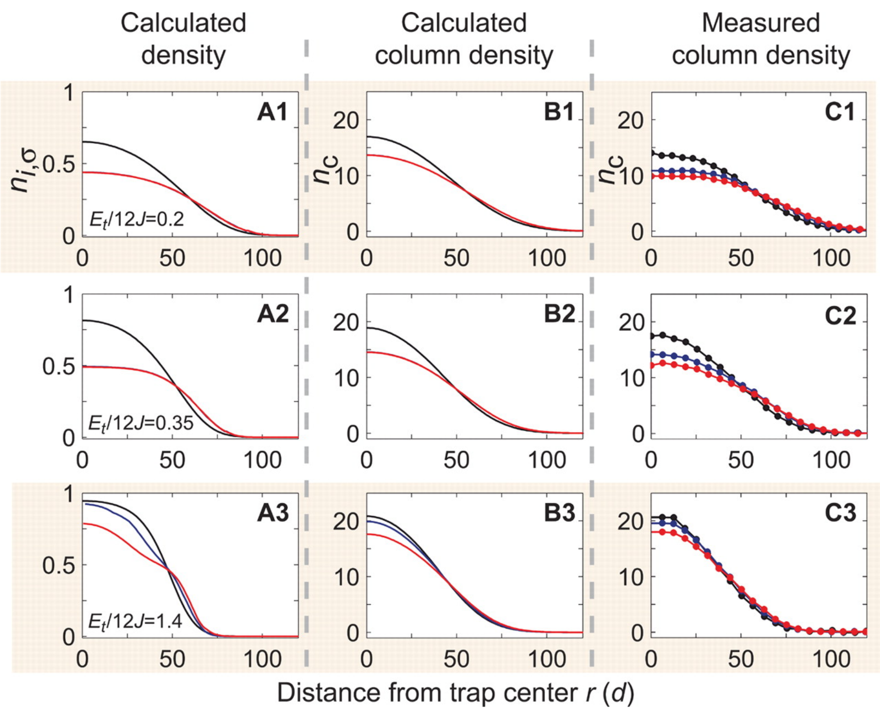

[Schneider et al, Science **322**, 1520 (2008)]

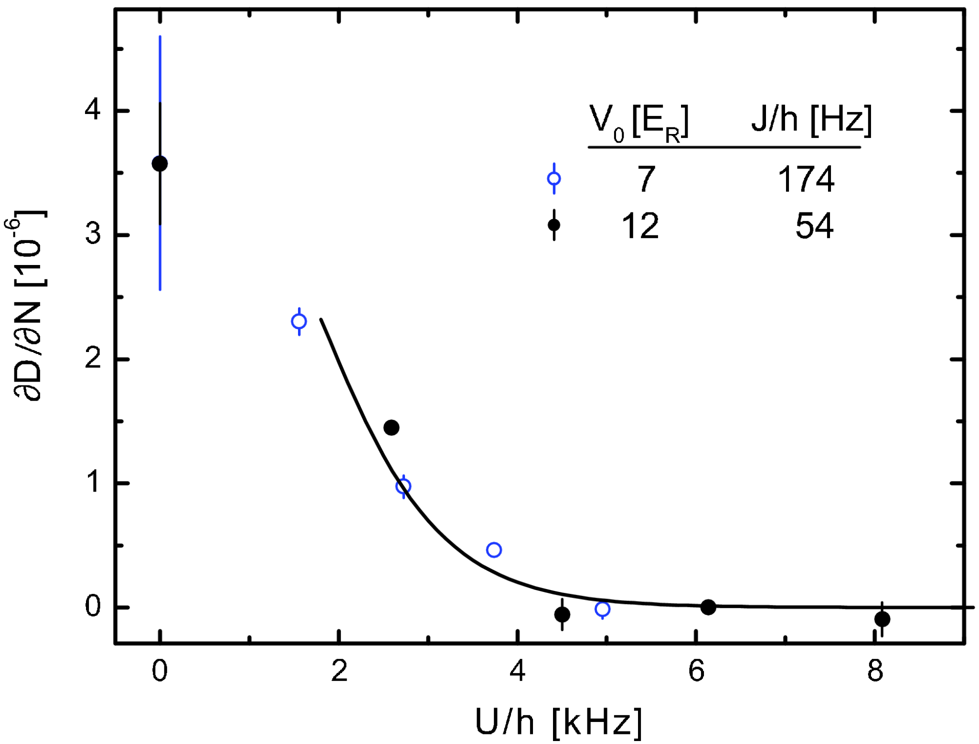

[Jördens et al., Nature (2008)]

Further MIT observables: column density, fraction of atoms with double occupations

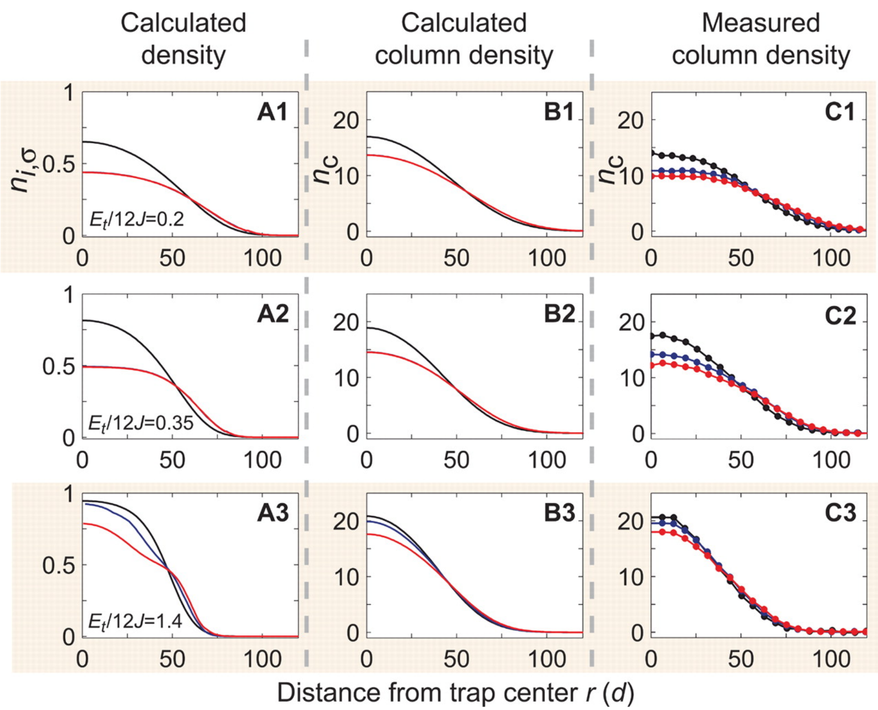

[Schneider et al, Science **322**, 1520 (2008)]

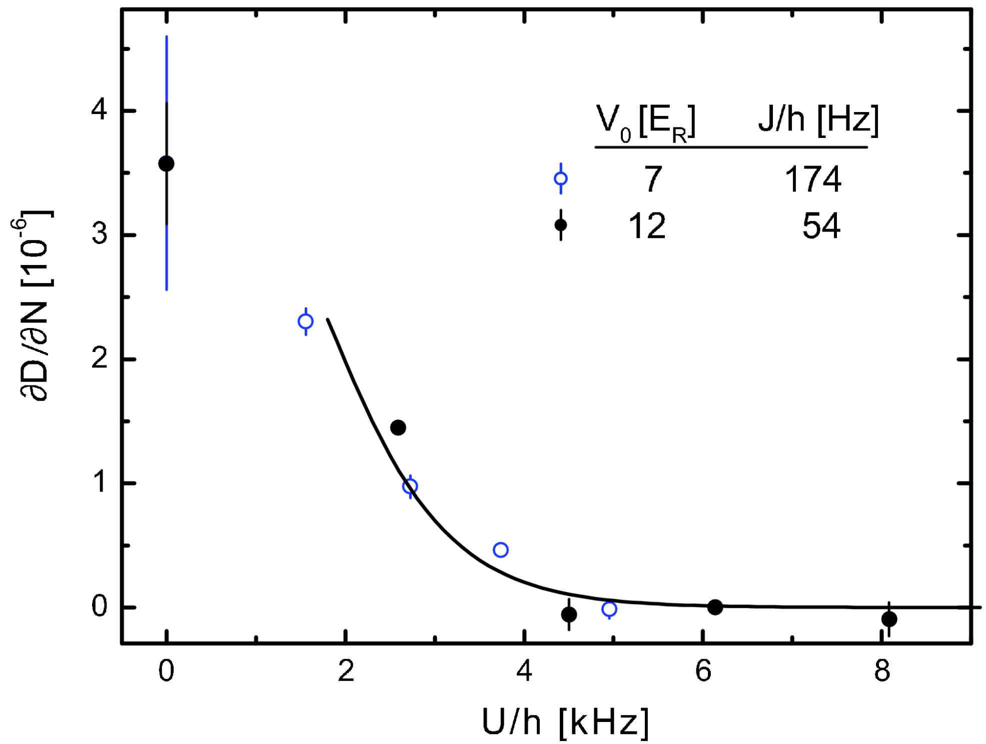

[Jördens et al., Nature (2008)]

Many other phenomena seen: superconductivity, vortices, BEC-BCS crossover, . . .

Next grand challenges:

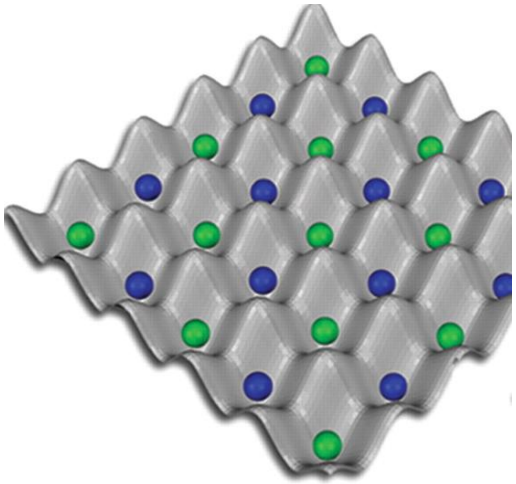

Antiferromagnetism (staggered order) in ultracold fermions

Problems:

(i) difficult to reach sufficiently low temperatures/entropies

(ii) detection of order parameter is not straightforward

Next grand challenges:

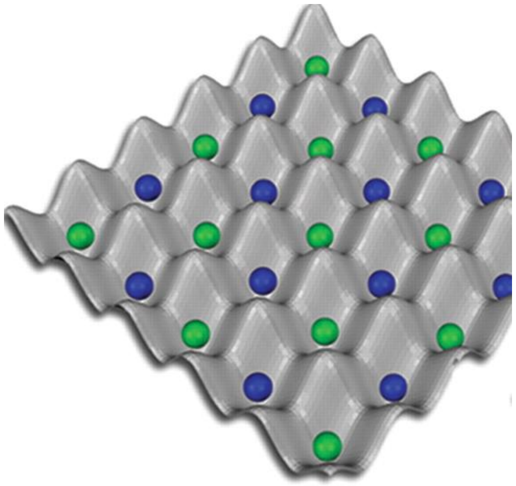

Antiferromagnetism (staggered order) in ultracold fermions

Problems:

(i) difficult to reach sufficiently low temperatures/entropies

(ii) detection of order parameter is not straightforward

Multiflavor phenomena, e.g. trions versus color superconductivity

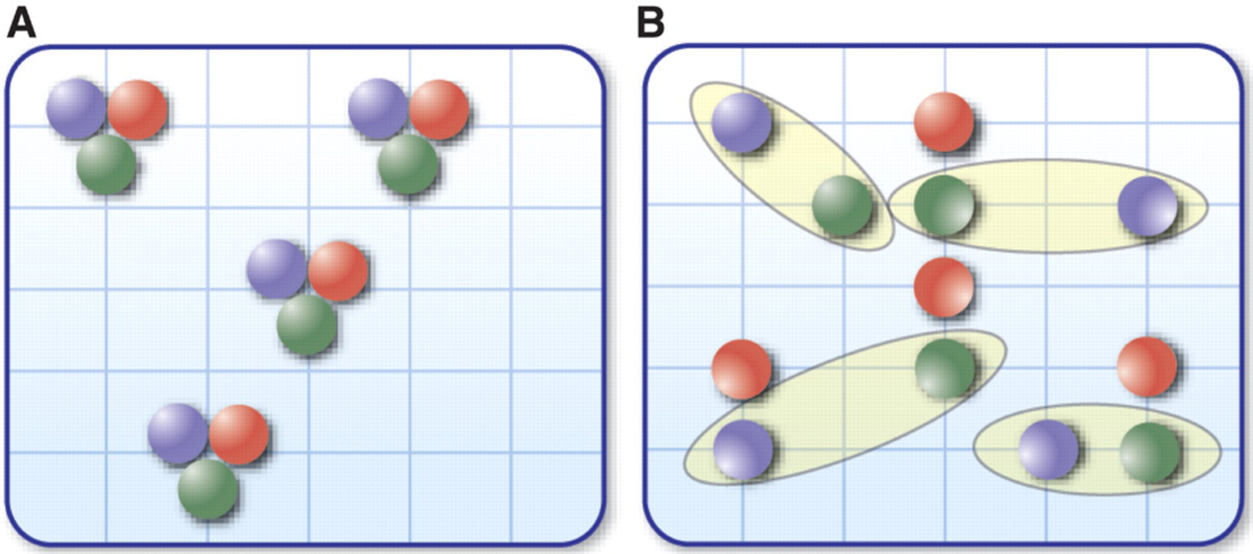

Approaches for correlated lattice Fermi systems

$$H = \sum_{i=1}^{N_e} \frac{\mathbf{p}_i^2}{2m} + \sum_i V(\mathbf{r}_i) + \sum_{i<j} \frac{e^2}{|\mathbf{r}_i - \mathbf{r}_j|}$$

reduction to valence electrons $\downarrow$

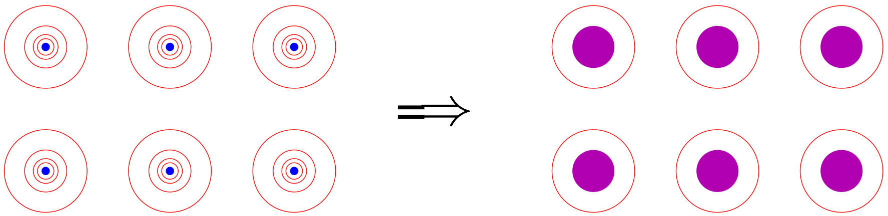

$$H = \sum_{i=1}^{N_v} \frac{\mathbf{p}_i^2}{2m} + \sum_{i=1}^{N_v} V^{\text{ion}}(\mathbf{r}_i) + \sum_{i=1}^{N_v-1} \sum_{j=i+1}^{N_v} V^{ee}(\mathbf{r}_i, \mathbf{r}_j)$$

Approaches for correlated lattice Fermi systems

$$H = \sum_{i=1}^{N_e} \frac{\boldsymbol{p}_i{}^2}{2m} + \sum_i V(\boldsymbol{r}_i) + \sum_{i<j} \frac{e^2}{|\boldsymbol{r}_i - \boldsymbol{r}_j|}$$

reduction to valence electrons ↓

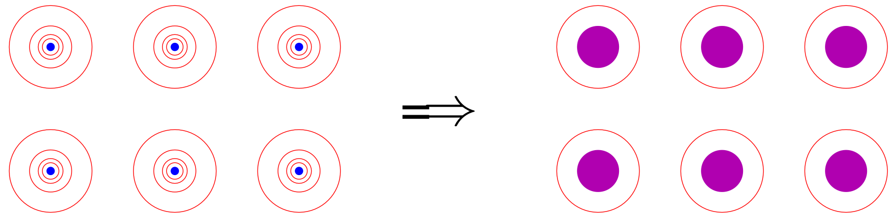

$$H = \sum_{i=1}^{N_v} \frac{\boldsymbol{p}_i^2}{2m} + \sum_{i=1}^{N_v} V^{\text{ion}}(\boldsymbol{r}_i) + \sum_{i=1}^{N_v-1} \sum_{j=i+1}^{N_v} V^{ee}(\boldsymbol{r}_i, \boldsymbol{r}_j)$$

occupation number formalism ↓ Wannier orbitals

$$\hat{H} = \sum_{i\nu j\sigma} t_{ij}^{\nu}\, \hat{c}_{i\nu\sigma}^{\dagger}\, \hat{c}_{j\nu\sigma} + \frac{1}{2} \sum_{\nu\nu'\mu\mu'} \sum_{ijmn} \sum_{\sigma\sigma'} \mathcal{V}_{ijmn}^{\nu\nu'\mu\mu'}\, \hat{c}_{i\nu\sigma}^{\dagger}\, \hat{c}_{j\nu'\sigma'}^{\dagger}\, \hat{c}_{n\mu'\sigma'}\, \hat{c}_{m\mu\sigma}$$

Approaches for correlated lattice Fermi systems

$$H = \sum_{i=1}^{N_e} \frac{\boldsymbol{p}_i^{\,2}}{2m} + \sum_i V(\boldsymbol{r}_i) + \sum_{i<j} \frac{e^2}{|\boldsymbol{r}_i - \boldsymbol{r}_j|}$$

reduction to valence electrons ↓

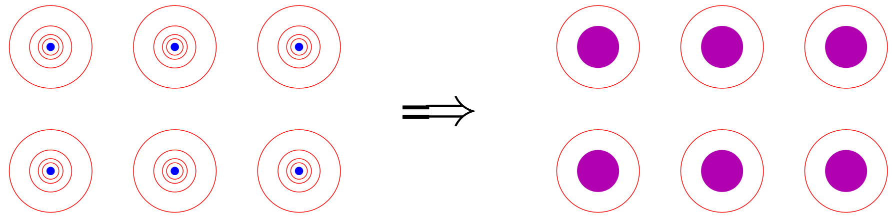

$$H = \sum_{i=1}^{N_v} \frac{\boldsymbol{p}_i^2}{2m} + \sum_{i=1}^{N_v} V^{\text{ion}}(\boldsymbol{r}_i) + \sum_{i=1}^{N_v-1} \sum_{j=i+1}^{N_v} V^{ee}(\boldsymbol{r}_i, \boldsymbol{r}_j)$$

occupation number formalism ↓ Wannier orbitals

$$\hat{H} = \sum_{i\nu j\sigma} t_{ij}^{\nu}\, \hat{c}_{i\nu\sigma}^{\dagger}\, \hat{c}_{j\nu\sigma} + \frac{1}{2} \sum_{\nu\nu'\mu\mu'} \sum_{ijmn} \sum_{\sigma\sigma'} \mathcal{V}_{ijmn}^{\nu\nu'\mu\mu'}\, \hat{c}_{i\nu\sigma}^{\dagger}\, \hat{c}_{j\nu'\sigma'}^{\dagger}\, \hat{c}_{n\mu'\sigma'}\, \hat{c}_{m\mu\sigma}$$

Hubbard model $$\hat{H} = \sum_{(i,j),\sigma} t_{ij}\, (\hat{c}_{i\sigma}^{\dagger} \hat{c}_{j\sigma} + \text{h.c.}) + U \sum_i \hat{n}_{i\uparrow} \hat{n}_{i\downarrow}$$

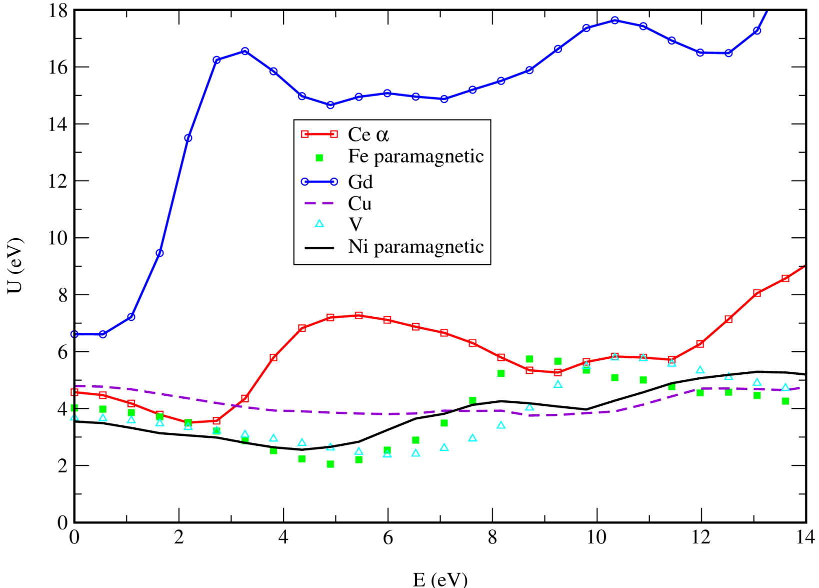

elated lattice Fermi systems

$$+ \sum_i V(\mathbf{r}_i) + \sum_{i<j} \frac{e^2}{|\mathbf{r}_i - \mathbf{r}_j|}$$

rons ↓

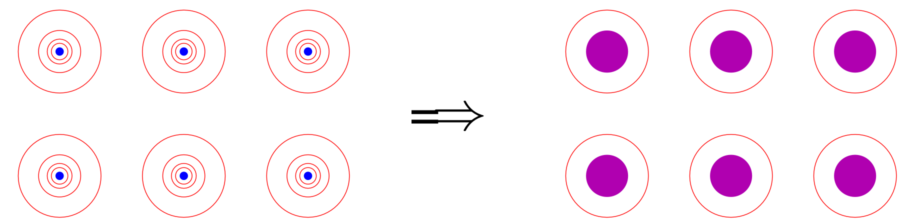

[Aryasetiawan et al, PRB 2006]

$$H = \sum_{i=1}^{N_v} \frac{\mathbf{p}_i^2}{2m} + \sum_{i=1}^{N_v} V^{\text{ion}}(\mathbf{r}_i) + \sum_{i=1}^{N_v-1} \sum_{j=i+1}^{N_v} V^{ee}(\mathbf{r}_i, \mathbf{r}_j)[\omega]$$

occupation number formalism ↓ Wannier orbitals

$$\hat{H} = \sum_{i\nu j\sigma} t_{ij}^{\nu}\, \hat{c}_{i\nu\sigma}^{\dagger}\, \hat{c}_{j\nu\sigma} + \frac{1}{2} \sum_{\nu\nu'\mu\mu'} \sum_{ijmn} \sum_{\sigma\sigma'} \mathcal{V}_{ijmn}^{\nu\nu'\mu\mu'}\, \hat{c}_{i\nu\sigma}^{\dagger}\, \hat{c}_{j\nu'\sigma'}^{\dagger}\, \hat{c}_{n\mu'\sigma'}\, \hat{c}_{m\mu\sigma}$$

Hubbard model $\hat{H} = \sum_{(i,j),\sigma} t_{ij}\, (\hat{c}_{i\sigma}^{\dagger} \hat{c}_{j\sigma} + \text{h.c.}) + U \sum_i \hat{n}_{i\uparrow} \hat{n}_{i\downarrow}$

elated lattice Fermi systems

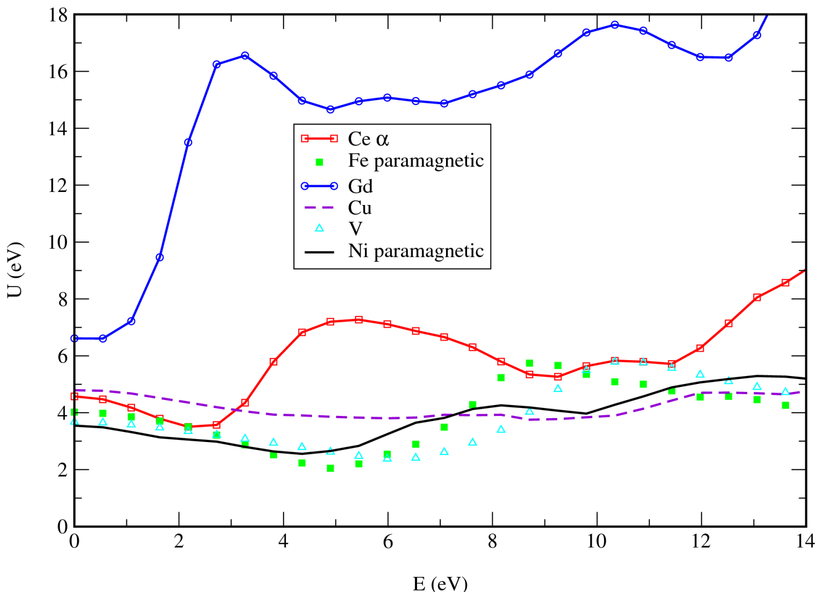

[Aryasetiawan et al, PRB 2006]

$$+ \sum_i V(\boldsymbol{r}_i) + \sum_{i<j} \frac{e^2}{|\boldsymbol{r}_i - \boldsymbol{r}_j|}$$

rons

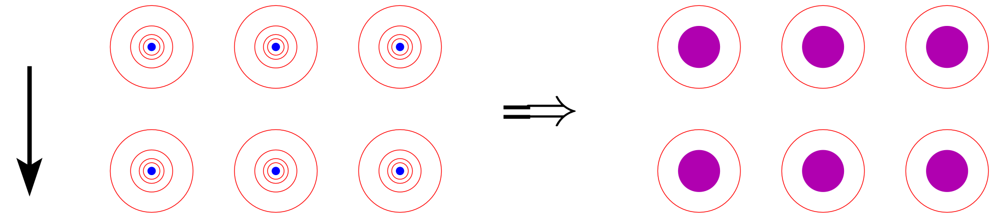

$$H = \sum_{i=1}^{N_v} \frac{\boldsymbol{p}_i^2}{2m} + \sum_{i=1}^{N_v} V^{\text{ion}}(\boldsymbol{r}_i) + \sum_{i=1}^{N_v-1} \sum_{j=i+1}^{N_v} V^{ee}(\boldsymbol{r}_i, \boldsymbol{r}_j)[\omega]$$

occupation number formalism ↓ Wannier orbitals

$$\hat{H} = \sum_{i\nu j\sigma} t_{ij}^{\nu} \hat{c}_{i\nu\sigma}^{\dagger} \hat{c}_{j\nu\sigma} + \frac{1}{2} \sum_{\nu\nu'\mu\mu'} \sum_{ijmn} \sum_{\sigma\sigma'} \mathcal{V}_{ijmn}^{\nu\nu'\mu\mu'} \hat{c}_{i\nu\sigma}^{\dagger} \hat{c}_{j\nu'\sigma'}^{\dagger} \hat{c}_{n\mu'\sigma'} \hat{c}_{m\mu\sigma}$$

Hubbard model $\hat{H} = \sum_{(i,j),\sigma} t_{ij} (\hat{c}_{i\sigma}^{\dagger} \hat{c}_{j\sigma} + \text{h.c.}) + U \sum_i \hat{n}_{i\uparrow} \hat{n}_{i\downarrow}$

Note: no core states in quantum gas case!

Approaches for Hubbard-type models

$$\hat{H} = \sum_{(i,j),\sigma} t_{ij} \, (\hat{c}^\dagger_{i\sigma} \hat{c}_{j\sigma} + \text{h.c.}) + U \sum_{i} \hat{n}_{i\uparrow} \hat{n}_{i\downarrow}$$

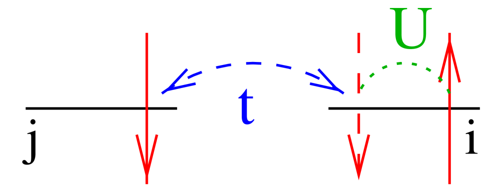

Perturbation theory

- $U \longrightarrow 0$: Hartree-Fock
  2^{nd} order PT, . . .
- $t/U \longrightarrow 0$ (for $n = 1$)
  $\rightsquigarrow$ Heisenberg model

finite clusters: ED, QMC

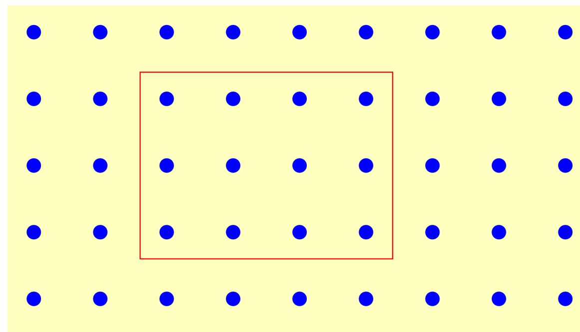

$d \rightarrow 1$: Bethe ansatz, DMRG

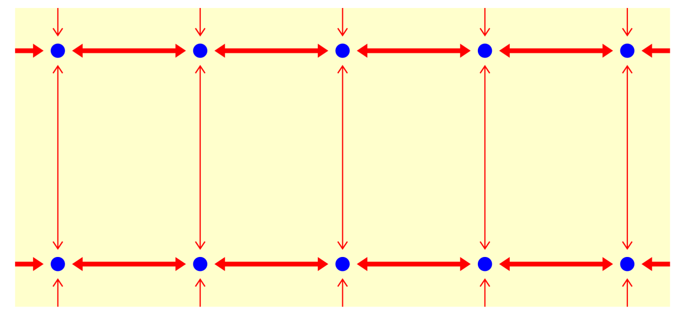

Approaches for Hubbard-type models

$$\hat{H} = \sum_{(i,j),\sigma} t_{ij} \, (\hat{c}^{\dagger}_{i\sigma} \hat{c}_{j\sigma} + \text{h.c.}) + U \sum_{i} \hat{n}_{i\uparrow} \hat{n}_{i\downarrow}$$

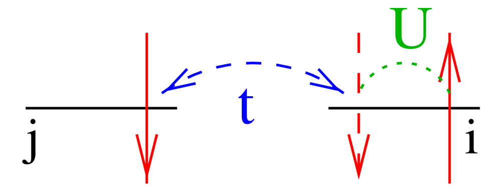

Perturbation theory

- $U \to 0$: Hartree-Fock
  2nd order PT, . . .
- $t/U \to 0$ (for $n = 1$)
  $\rightsquigarrow$ Heisenberg model

finite clusters: ED, QMC

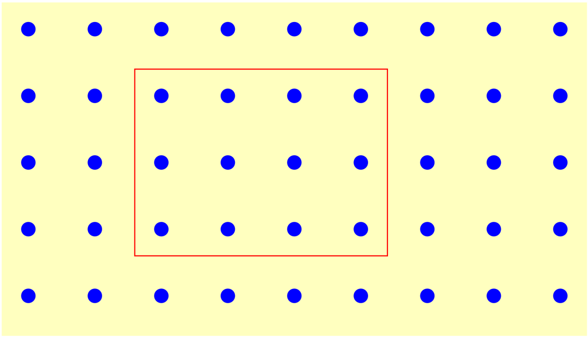

$d \to 1$: Bethe ansatz, DMRG

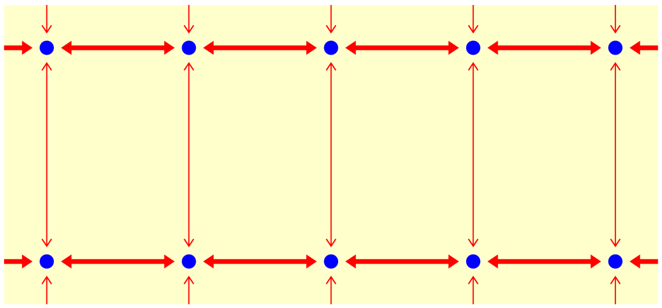

Dynamical mean-field theory (DMFT): local self-energy $\Sigma(\boldsymbol{k}, \omega) \equiv \Sigma(\omega)$

[Metzner, Vollhardt, PRL (1989), Georges, Kotliar, PRL (1992), Jarrell, PRL (1992)]

+ non-perturbative $\rightsquigarrow$ valid at MIT
+ dynamical on-site correlations preserved
+ in thermodynamic limit

+/− exact for coordination $Z \to \infty$

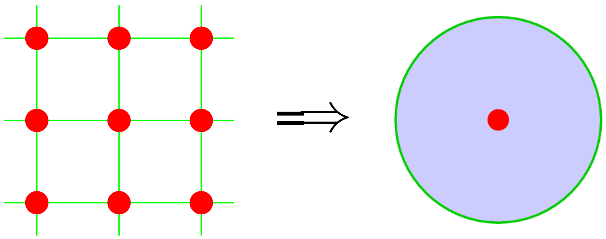

Iterative solution of DMFT equations

0. Initialize self-energy
1. Solve Dyson equation
2. Solve single impurity Anderson model (SIAM)

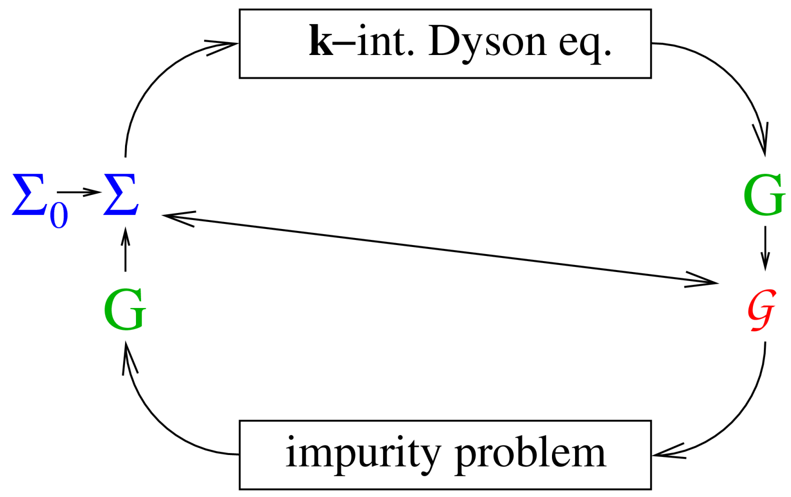

$\longleftarrow$ DOS / t_{ij} / $\varepsilon_{\nu\boldsymbol{k}}$

$\longleftarrow$ local interactions

Iterative solution of DMFT equations

0. Initialize self-energy
1. Solve Dyson equation
2. Solve single impurity Anderson model (SIAM)

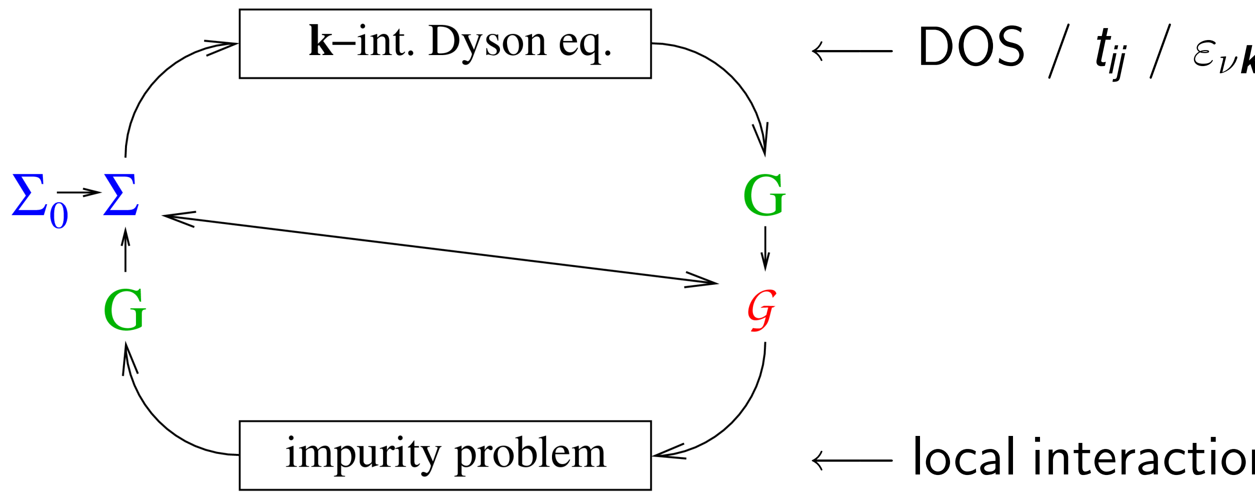

Impurity solver:

- Iterative perturbation theory (IPT; not controlled)
- Quantum Monte Carlo (QMC)
- Exact diagonalization (ED; large finite-size errors)
- Numerical renormalization group (NRG; 1-2 bands)
- Density matrix renormalization group (DMRG)
- Self-energy functional theory (SFT) + ED

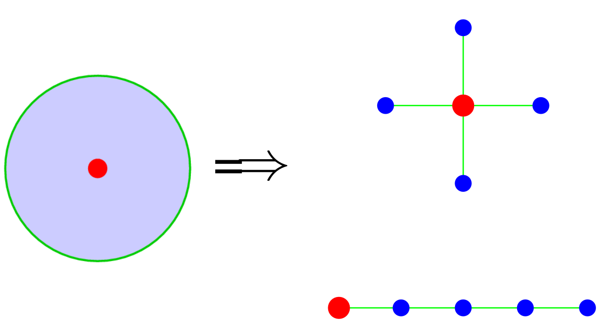

Auxiliary-field QMC algorithm [Hirsch, Fye (1986)]

Green function G in imaginary time (fermionic Grassmann variables ψ, ψ^*):

$$G_\sigma(\tau_2 - \tau_1) = \frac{1}{\mathcal{Z}} \int \mathcal{D}[\psi]\,\mathcal{D}[\psi^*]\;\; \psi_\sigma(\tau_1)\psi^*_\sigma(\tau_2)\;\; \exp\Big[\mathcal{A}_0 - U \sum_{\sigma\sigma'} \int_0^\beta d\tau\, \psi^*_\sigma \psi_\sigma \psi^*_{\sigma'} \psi_{\sigma'}\Big]$$

Auxiliary-field QMC algorithm [Hirsch, Fye (1986)]

Green function G in imaginary time (fermionic Grassmann variables ψ, ψ^*):

$$G_\sigma(\tau_2 - \tau_1) = \frac{1}{\mathcal{Z}} \int \mathcal{D}[\psi]\,\mathcal{D}[\psi^*]\;\; \psi_\sigma(\tau_1)\psi^*_\sigma(\tau_2)\;\exp\Big[\mathcal{A}_0 - U \sum_{\sigma\sigma'} \int_0^\beta d\tau\, \psi^*_\sigma \psi_\sigma \psi^*_{\sigma'} \psi_{\sigma'}\Big]$$

(i) Imaginary-time discretization $\beta = \Lambda\,\Delta\tau$

(ii) Trotter decoupling $e^{-\beta(\hat{T}+\hat{V})} \approx \left[e^{-\Delta\tau\hat{T}} e^{-\Delta\tau\hat{V}}\right]^\Lambda$

Auxiliary-field QMC algorithm [Hirsch, Fye (1986)]

Green function G in imaginary time (fermionic Grassmann variables ψ, ψ^*):

$$G_\sigma(\tau_2-\tau_1) = \frac{1}{\mathcal{Z}}\int \mathcal{D}[\psi]\,\mathcal{D}[\psi^*]\;\psi_\sigma(\tau_1)\psi^*_\sigma(\tau_2)\;\exp\left[\mathcal{A}_0 - U\sum_{\sigma\sigma'}\int_0^\beta d\tau\,\psi^*_\sigma\psi_\sigma\psi^*_{\sigma'}\psi_{\sigma'}\right]$$

(i) Imaginary-time discretization $\beta = \Lambda\,\Delta\tau$

(ii) Trotter decoupling $e^{-\beta(\hat{T}+\hat{V})} \approx \left[e^{-\Delta\tau\hat{T}}e^{-\Delta\tau\hat{V}}\right]^\Lambda$

(iii) Hubbard-Stratonovich transformation

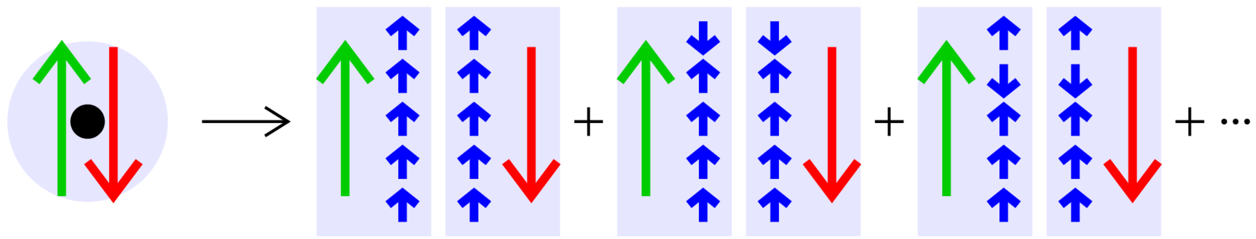

Wick theorem:

$$G = \frac{\sum M\det\{M\}}{\sum \det\{M\}}$$

Auxiliary-field QMC algorithm [Hirsch, Fye (1986)]

Green function G in imaginary time (fermionic Grassmann variables ψ, ψ^*):

$$G_\sigma(\tau_2 - \tau_1) = \frac{1}{\mathcal{Z}} \int \mathcal{D}[\psi]\,\mathcal{D}[\psi^*]\;\psi_\sigma(\tau_1)\psi^*_\sigma(\tau_2)\;\exp\Big[\mathcal{A}_0 - U \sum_{\sigma\sigma'} \int_0^\beta d\tau\, \psi^*_\sigma\psi_\sigma\psi^*_{\sigma'}\psi_{\sigma'}\Big]$$

(i) Imaginary-time discretization $\beta = \Lambda\,\Delta\tau$

(ii) Trotter decoupling $e^{-\beta(\hat{T}+\hat{V})} \approx \left[e^{-\Delta\tau\hat{T}}e^{-\Delta\tau\hat{V}}\right]^\Lambda$

(iii) Hubbard-Stratonovich transformation

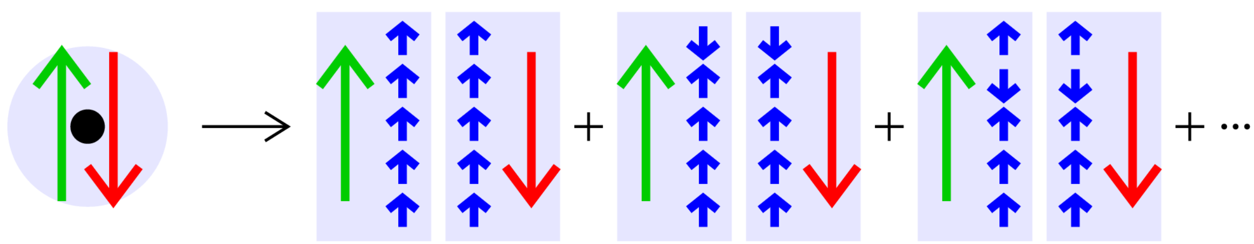

Wick theorem:

$$G = \frac{\sum M \det\{M\}}{\sum \det\{M\}}$$

(iv) MC importance sampling over auxiliary Ising field $\{s\}$: 2^Λ configurations

+ numerically exact, + no sign problem, (density-type interactions) − effort scales as T^{-3}

Multigrid Hirsch-Fye quantum Monte Carlo algorithm

State of the art: (a) conventional HF-QMC

(b) *a posteriori* extrapolation of selected observables

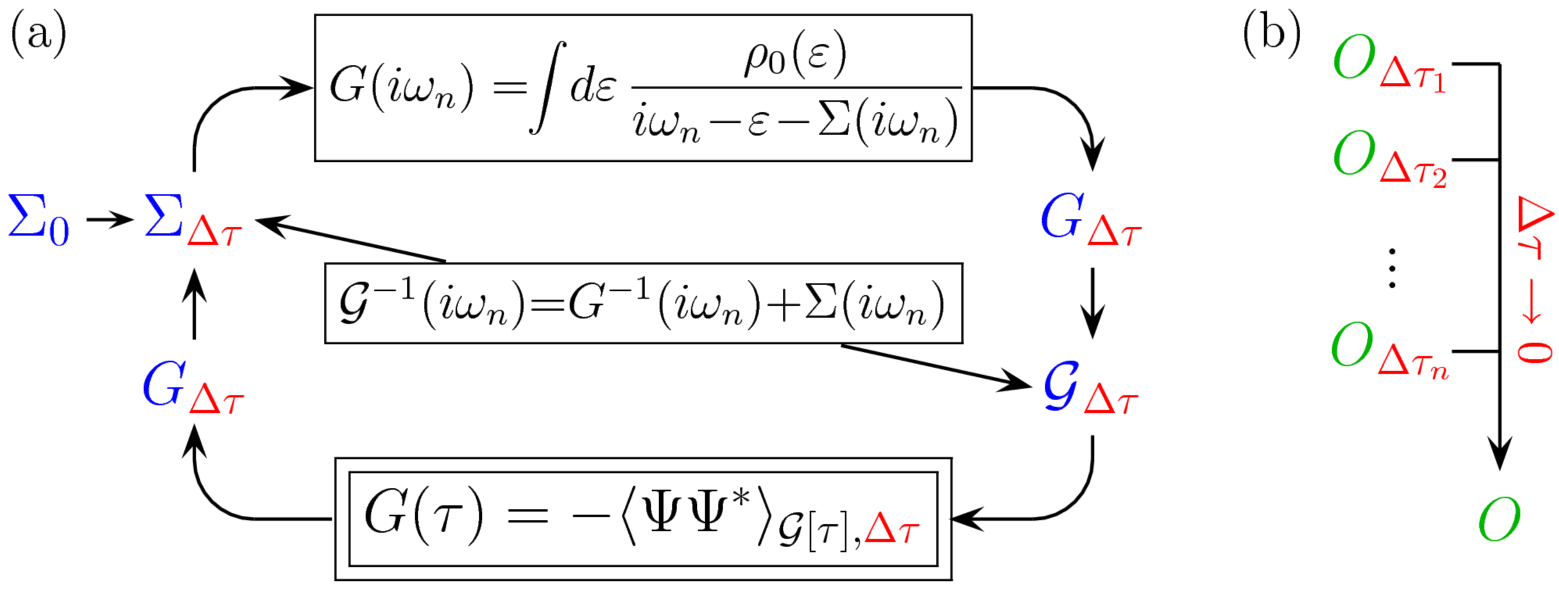

Multigrid Hirsch-Fye quantum Monte Carlo algorithm

State of the art: (a) conventional HF-QMC

(b) *a posteriori* extrapolation of selected observables

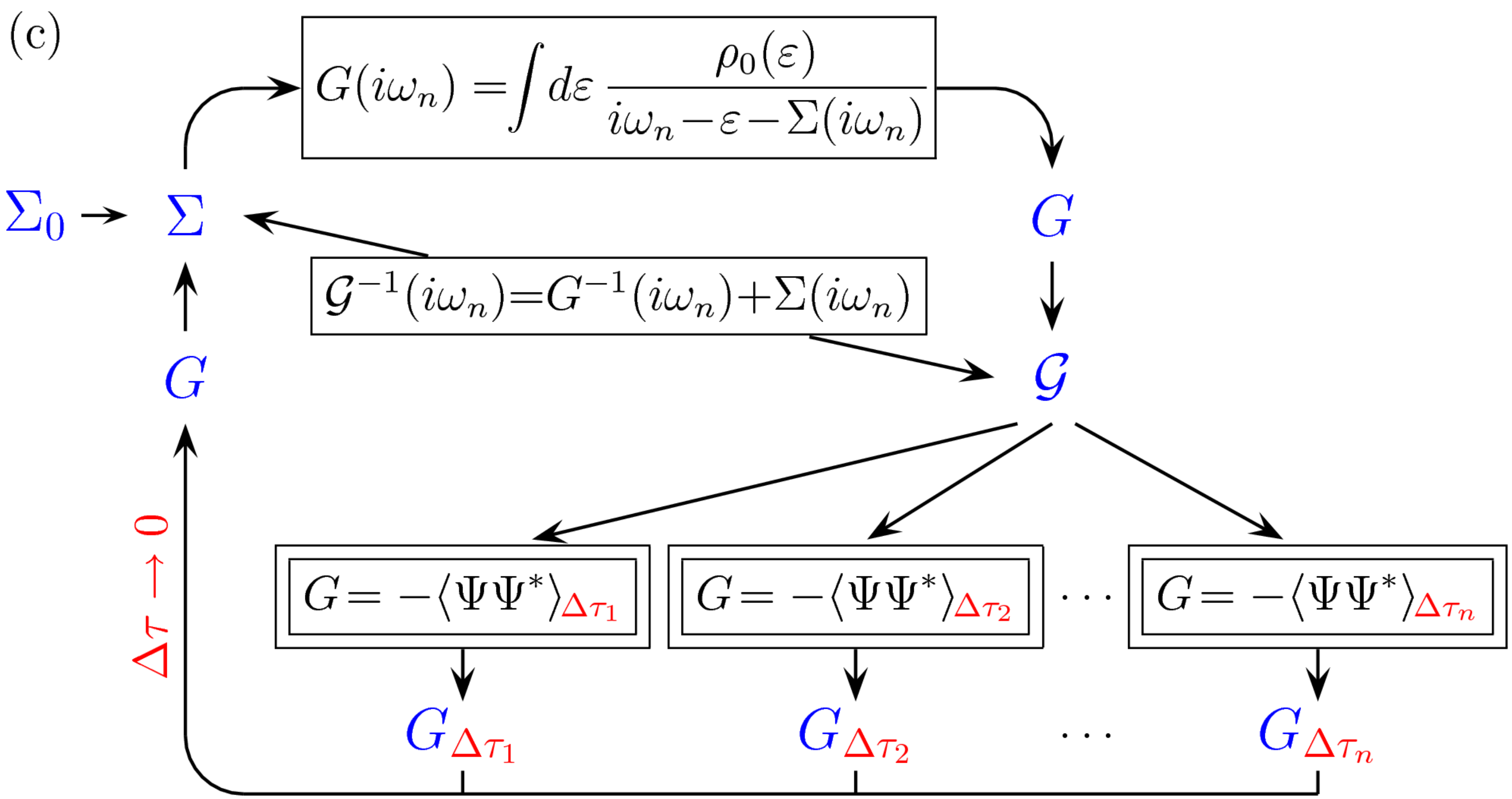

(c) Multigrid HF-QMC: internal elimination of Trotter error

$\rightsquigarrow$ quasi CT-QMC algorithm [NB, arXiv:0801.1222, PRA(2009)]

General method development: new initiative DFG-FG 1346

Positive evaluation on 2010/04/15+16, senate decision on 2010/06/30.

FOR 1346:
Dynamical Mean-Field Approach with Predictive Power for Strongly Correlated Materials

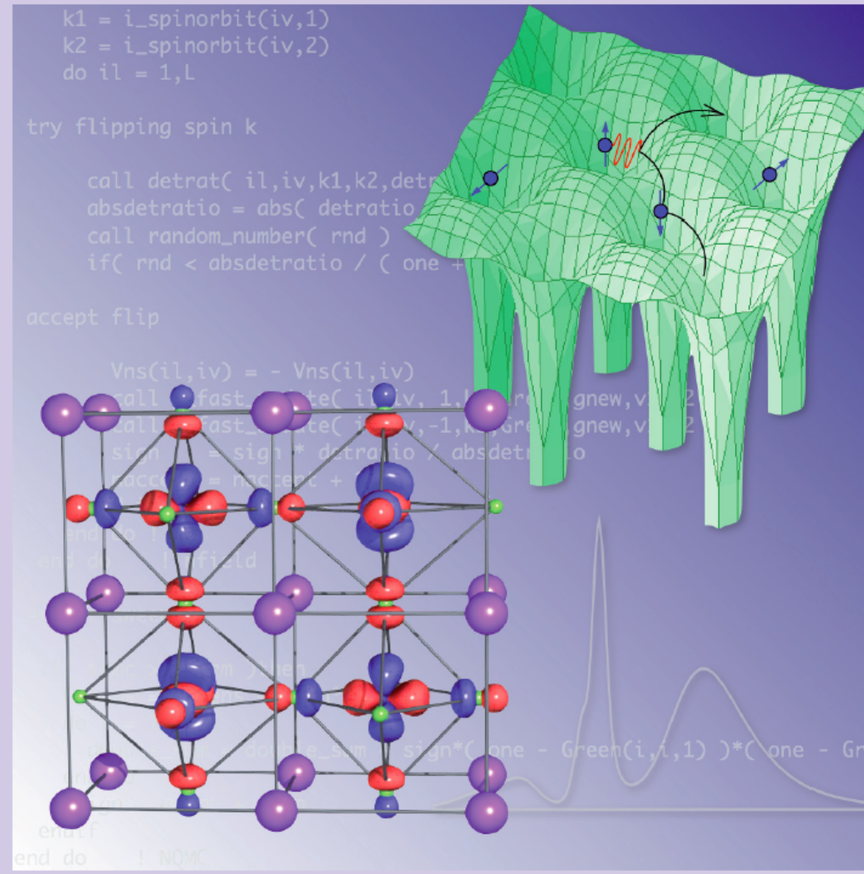

Dieter Vollhardt, University of Augsburg (Spokesperson)
Alexander Lichtenstein, University of Hamburg (Co-Spokesperson)

General method development: new initiative DFG-FG 1346

Positive evaluation on 2010/04/15+16, senate decision on 2010/06/30.

P8: Quantum Monte Carlo impurity solvers for multi-orbital problems and frequency-dependent interactions (F. Assaad, N. Blümer, P. Werner)

- determine most efficient QMC impurity solver for important problem classes
- study impact of neglected interactions
- generalize CT-QMC solvers for frequency-dependent interactions
- eliminate systematic errors in BSS solver (linear in $1/T$) using multigrid approach

FOR 1346:
Dynamical Mean-Field Approach with Predictive Power for Strongly Correlated Materials

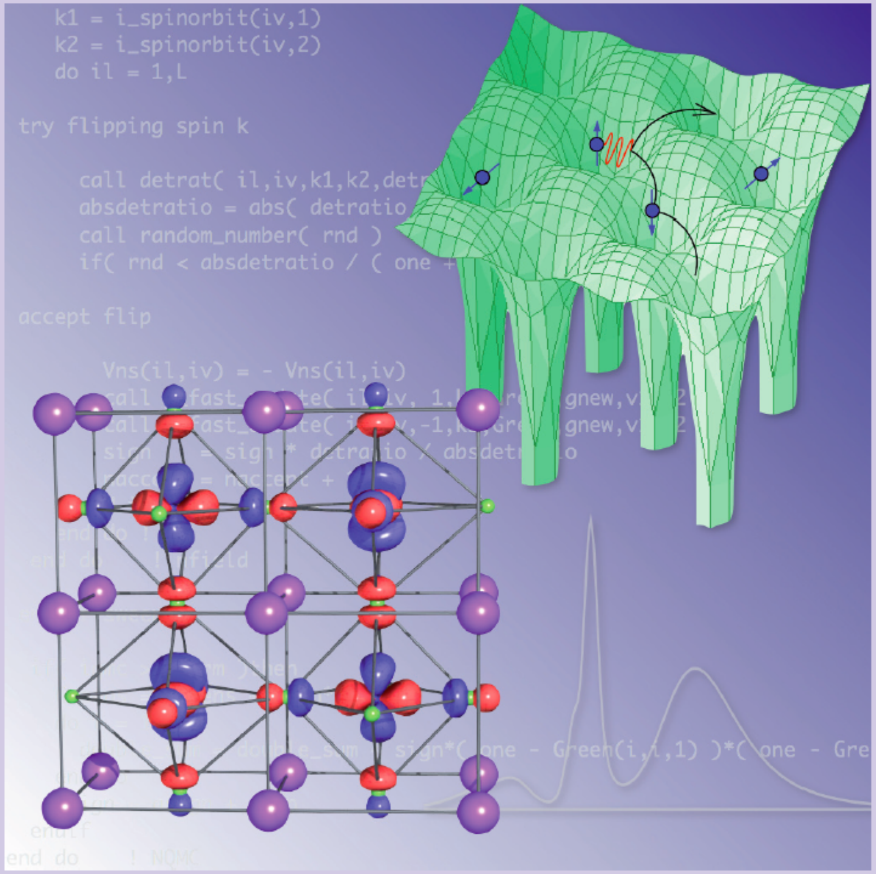

Dieter Vollhardt, University of Augsburg (Spokesperson)
Alexander Lichtenstein, University of Hamburg (Co-Spokesperson)

Paramagnetic Mott transitions in 3-flavor mixtures

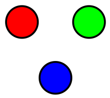

3 flavors: simplest case beyond electronic systems
1st approximation: all flavors equivalent

Paramagnetic Mott transitions in 3-flavor mixtures

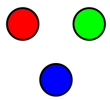

3 flavors: simplest case beyond electronic systems

1$^{\text{st}}$ approximation: all flavors equivalent

- Qualitatively new physics: $U < 0$, $n = 1.5$ [Hofstetter, PRB (2004), PRL (2007)]

  Color superconductivity

  Trionic phase

  . . .

Paramagnetic Mott transitions in 3-flavor mixtures

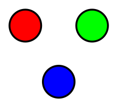

3 flavors: simplest case beyond electronic systems
1st approximation: all flavors equivalent

- Qualitatively new physics: $U < 0$, $n = 1.5$ [Hofstetter, PRB (2004), PRL (2007)]

  Color superconductivity
  Trionic phase
  . . .

- Ordered phases: $U > 0$, $n = 1$

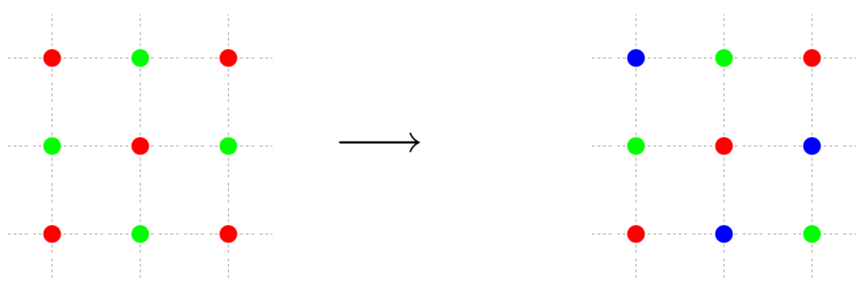

2 spins/flavors

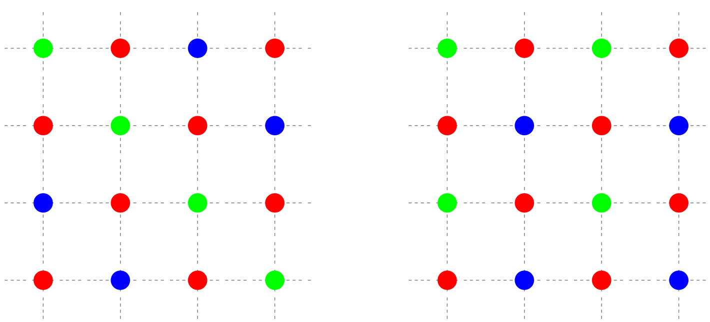

3 spins/flavors

Paramagnetic Mott transitions in 3-flavor mixtures

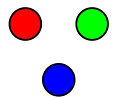

3 flavors: simplest case beyond electronic systems
1^{st} approximation: all flavors equivalent

- Qualitatively new physics: $U < 0$, $n = 1.5$ [Hofstetter, PRB (2004), PRL (2007)]

  Color superconductivity
  Trionic phase
  . . .

- Ordered phases: $U > 0$, $n = 1$

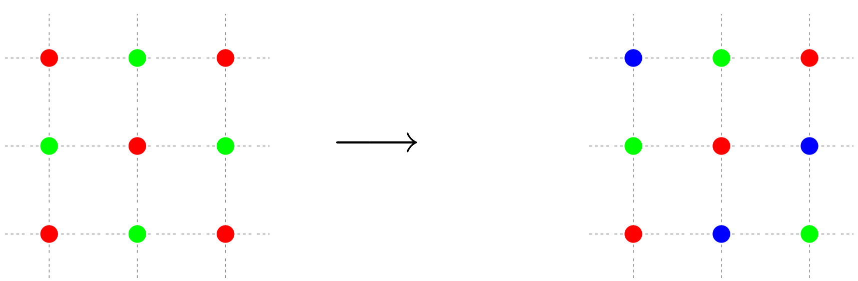

2 spins/flavors

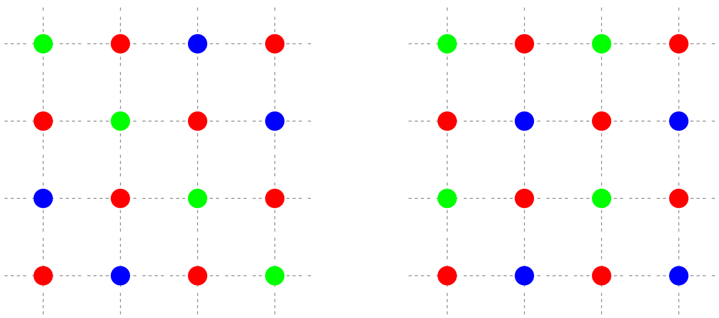

3 spins/flavors

Most "electron-like": $U > 0$, paramagnetic phase

Results at low T: particle density n and compressibility $\kappa = \frac{dn}{d\mu}$ (vs. μ)

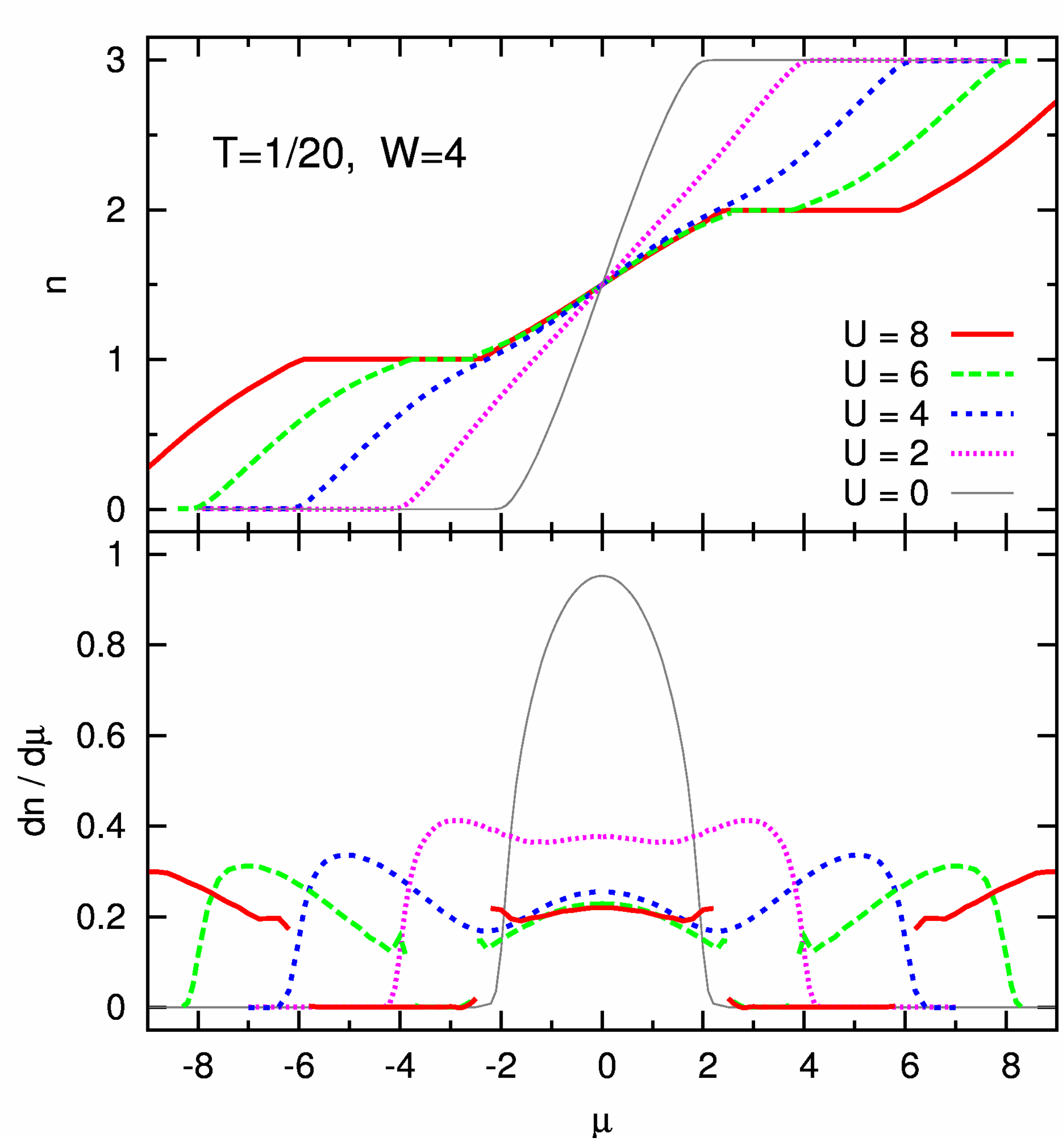

HF-QMC, Bethe DOS ($W = 4$)

Plateaus at integer filling ($U \gtrsim 5.5$)
$\rightsquigarrow$ incompressible Mott phases

[E. Gorelik, N. Blümer, PRA(2009)]

Results at low T: particle density n and compressibility $\kappa = \frac{dn}{d\mu}$ (vs. μ)

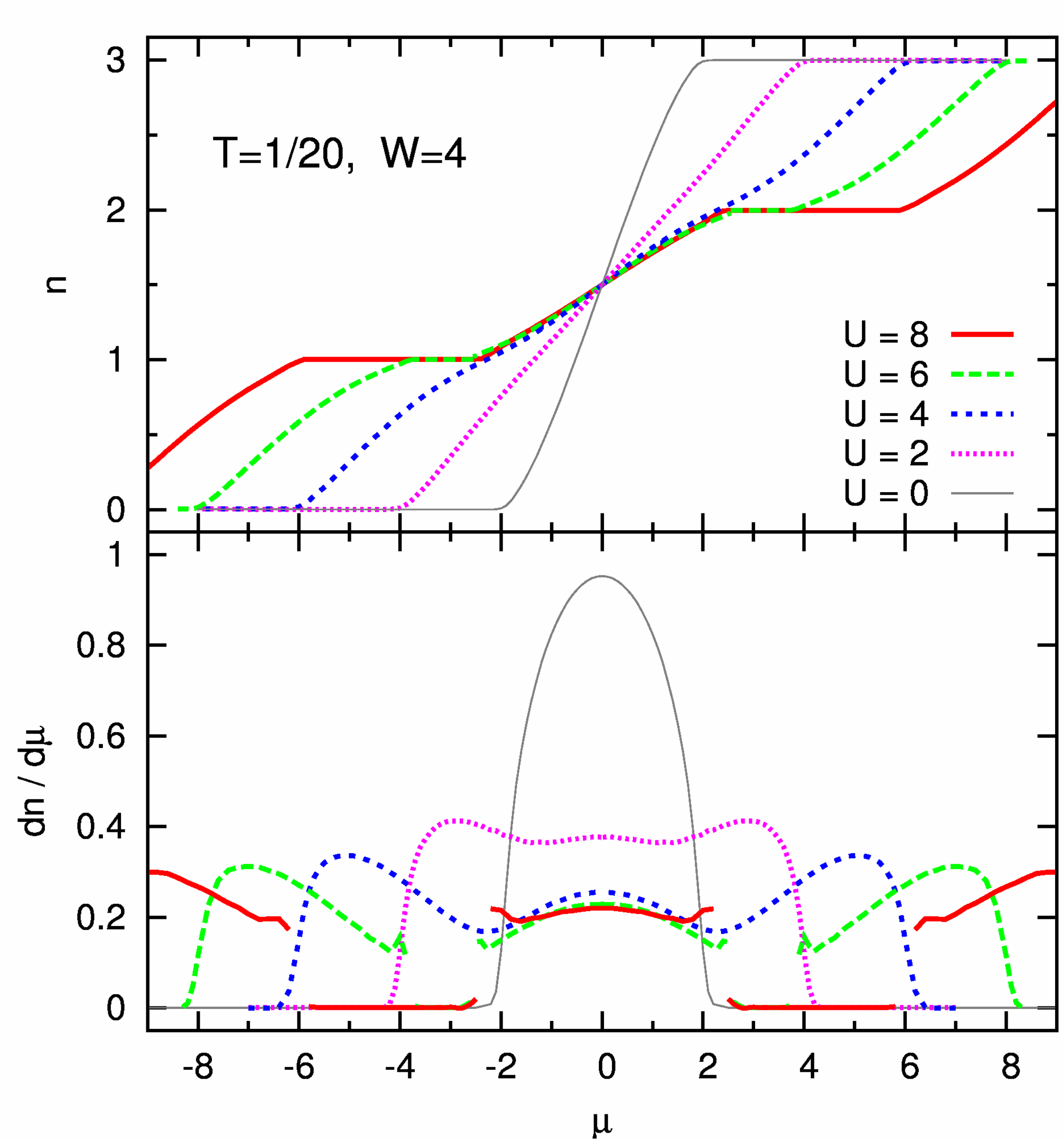

HF-QMC, Bethe DOS ($W = 4$)

Plateaus at integer filling ($U \gtrsim 5.5$)

$\rightsquigarrow$ incompressible Mott phases

$1 < n < 2$: semi-compressible phase

κ independent of μ, U, T

[E. Gorelik, N. Blümer, PRA(2009)]

Results at low T: particle density n and compressibility $\kappa = \frac{dn}{d\mu}$ (vs. μ)

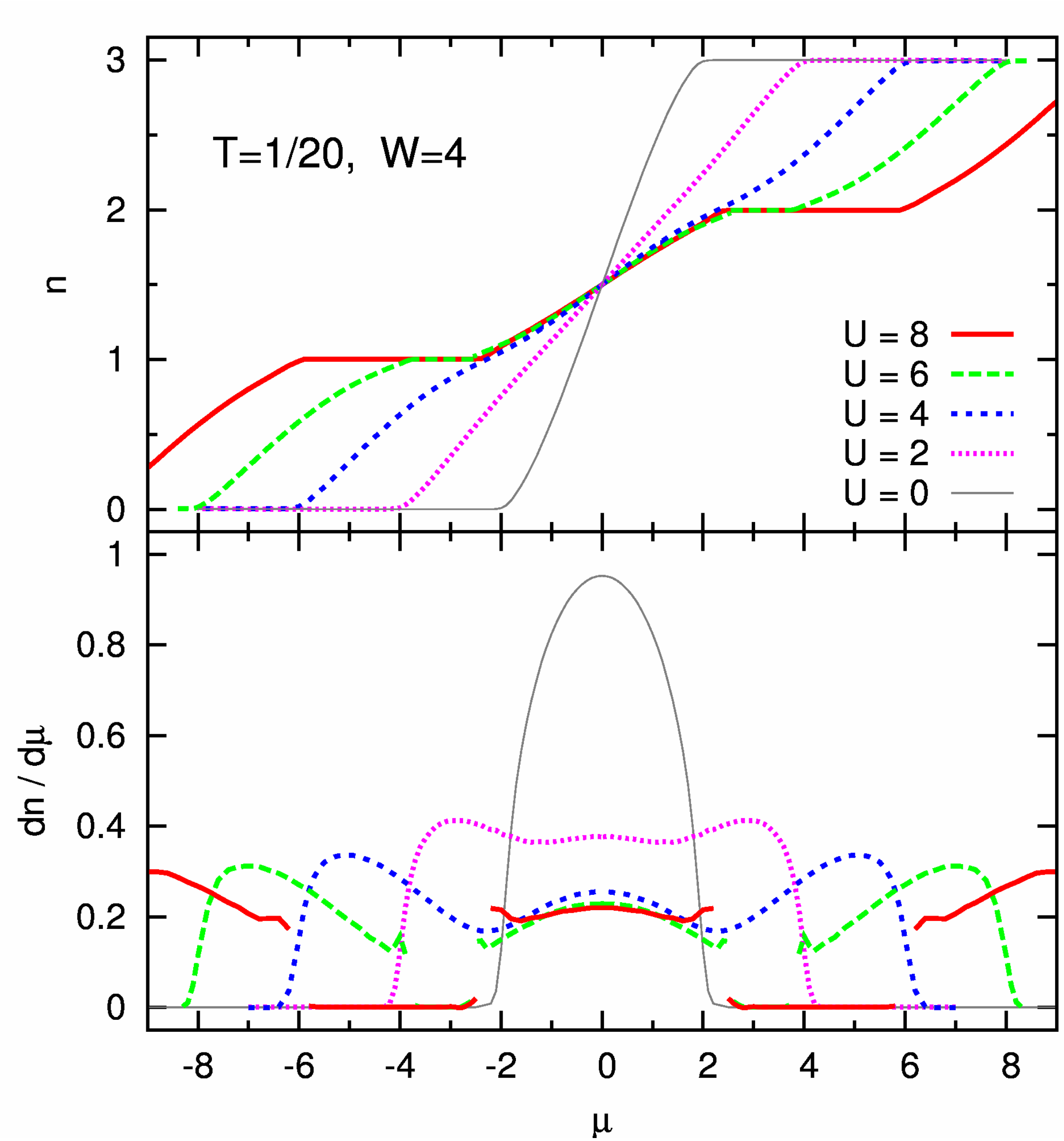

[E. Gorelik, N. Blümer, PRA(2009)]

HF-QMC, Bethe DOS ($W = 4$)

Plateaus at integer filling ($U \gtrsim 5.5$)

$\rightsquigarrow$ incompressible Mott phases

$1 < n < 2$: semi-compressible phase

κ independent of μ, U, T

Contrast with SU(4) system:

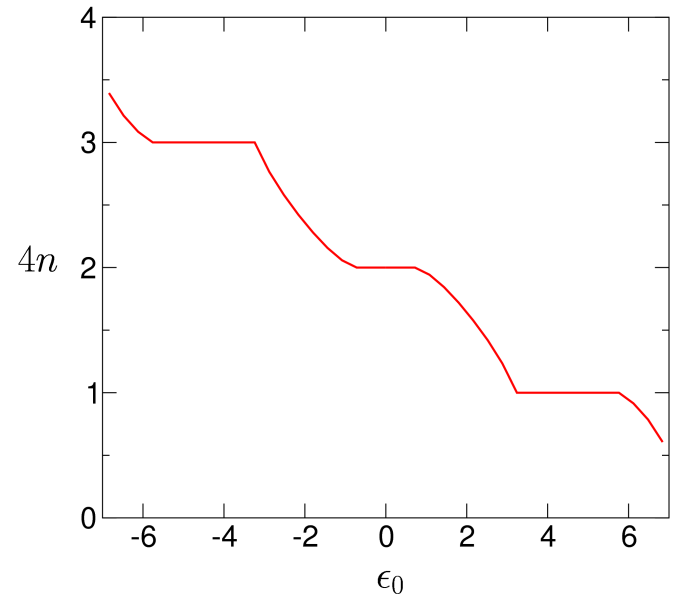

[Florens, Georges, PRB **70**, 035114 (2004)]

T dependence of density n and compressibility κ

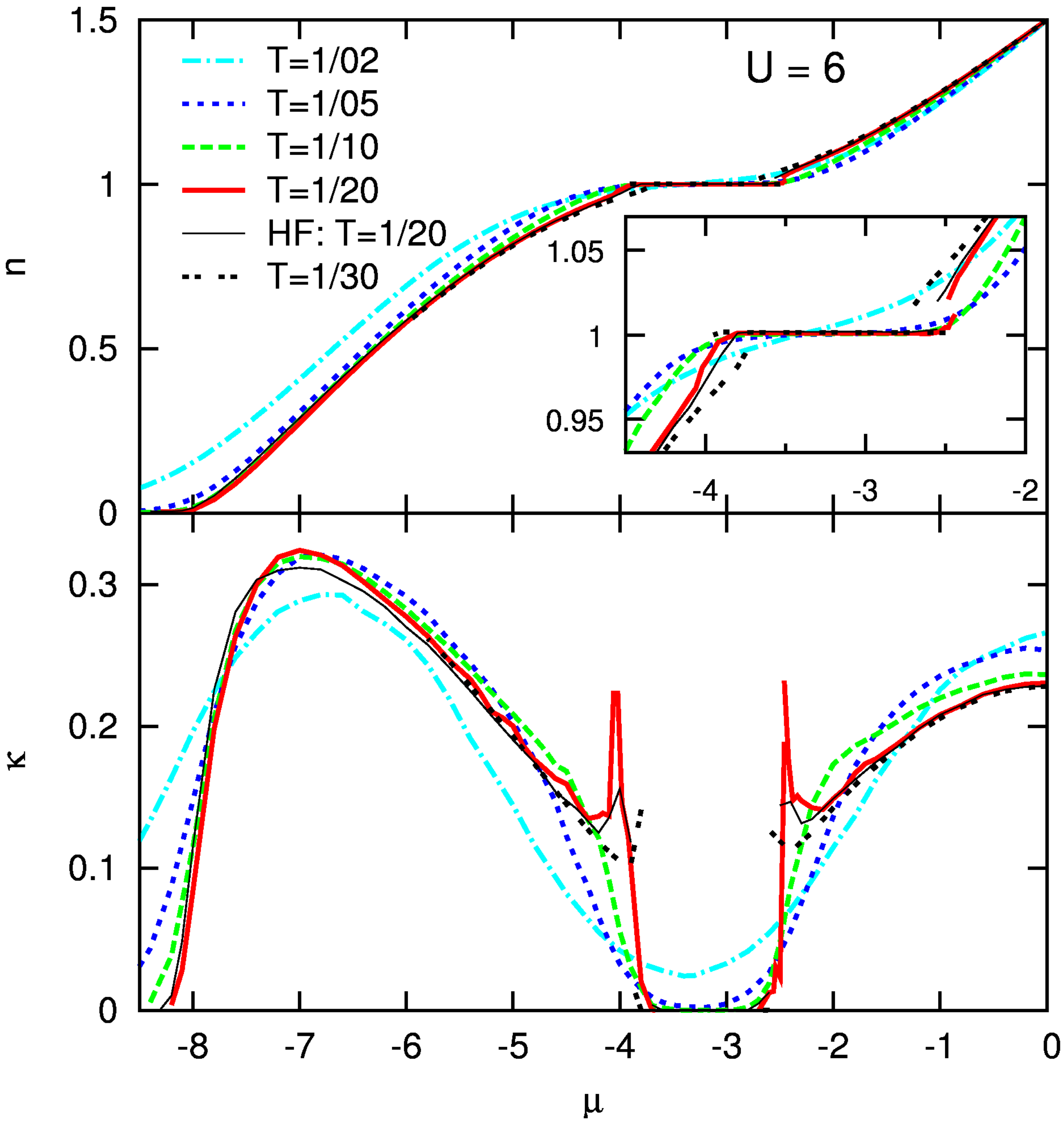

Multigrid HF-QMC results

(also HF-QMC at T = 1/20):

Critical temperature $T^* \approx 1/20$

T dependence of density n and compressibility κ

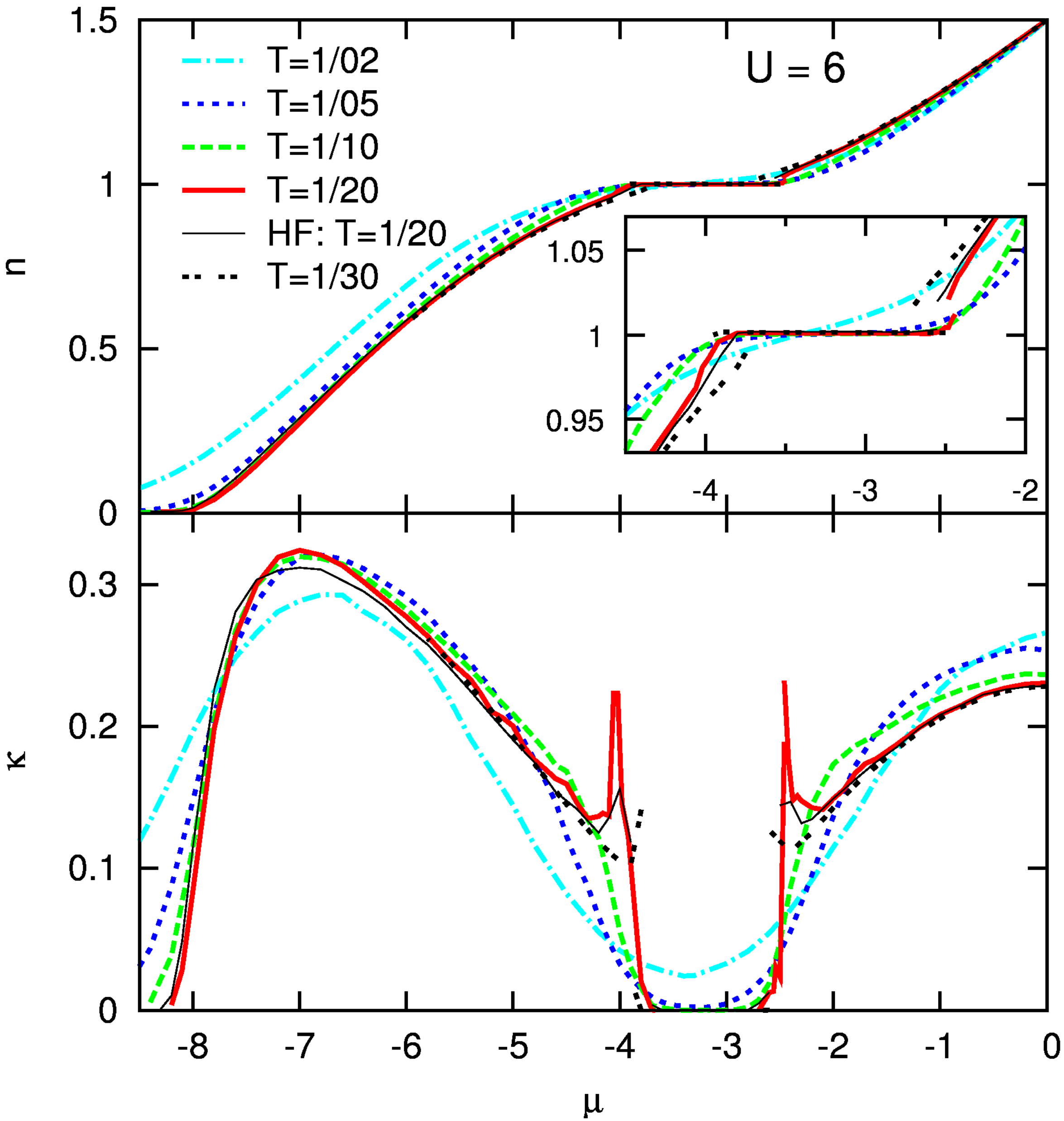

Multigrid HF-QMC results

(also HF-QMC at T = 1/20):

Critical temperature $T^{*} \approx 1/20$

Important for experiments:

Signatures of Mott transition persist to high temperatures:

nearly complete suppression of κ (at $n \approx 1$) up to $T \approx 1/5$.

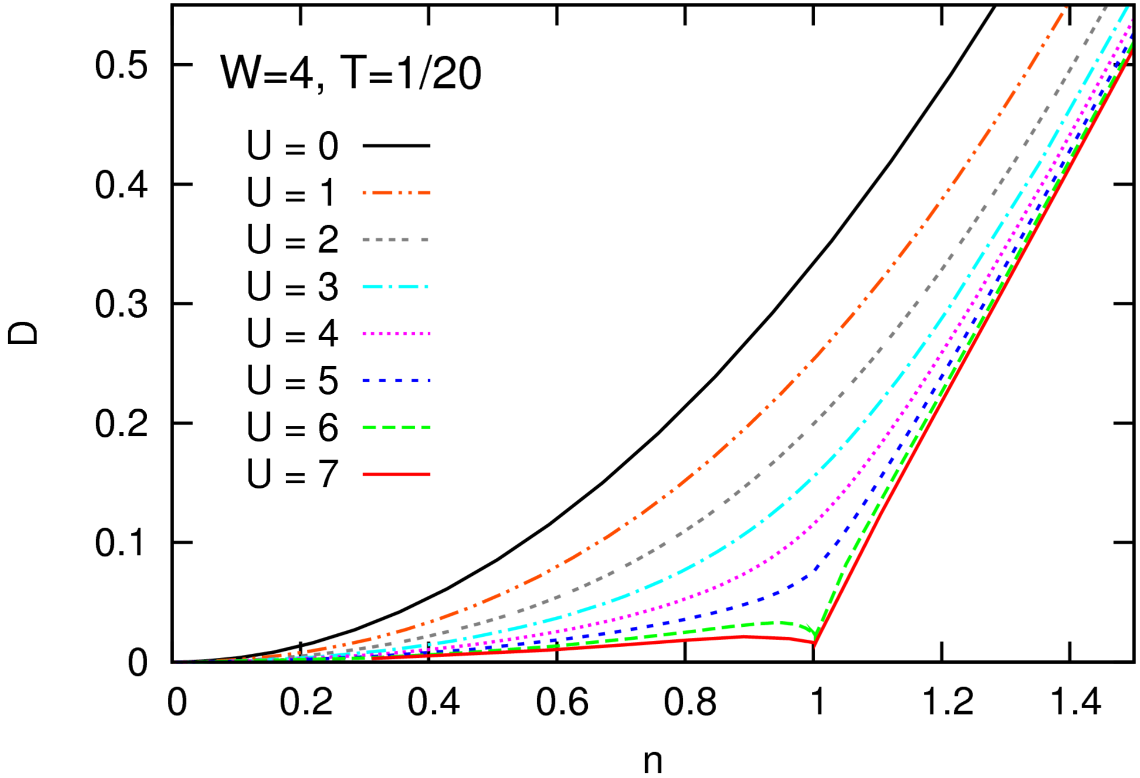

3-spin/flavor system:

Pair occupancy vs. density

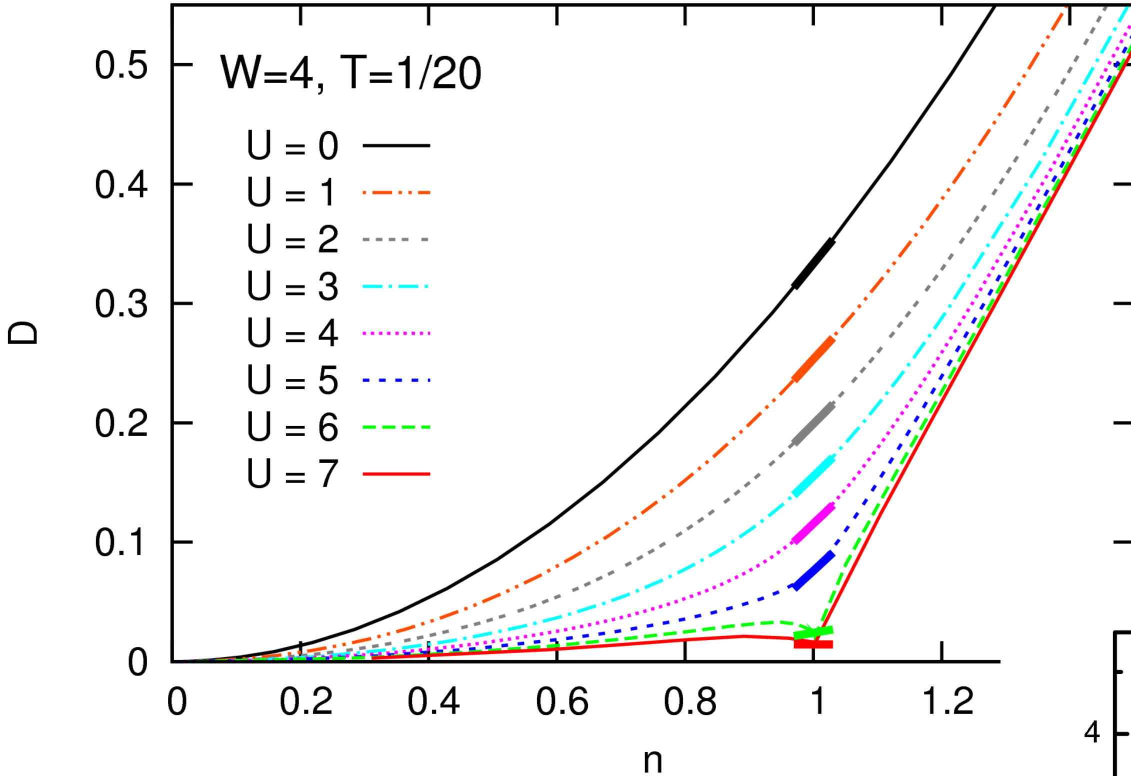

3-spin/flavor system:

Pair occupancy vs. density

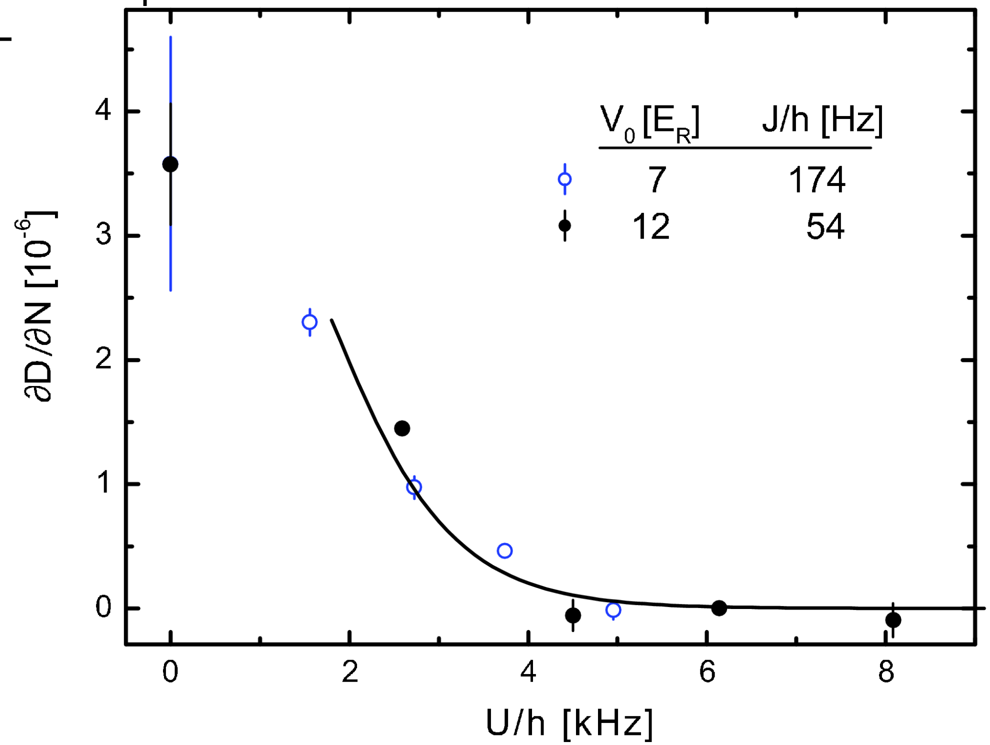

Experiment: 2-spin system

Transition to an incompressible phase

[Jördens et al., Nature (2008)]

Local spectral function

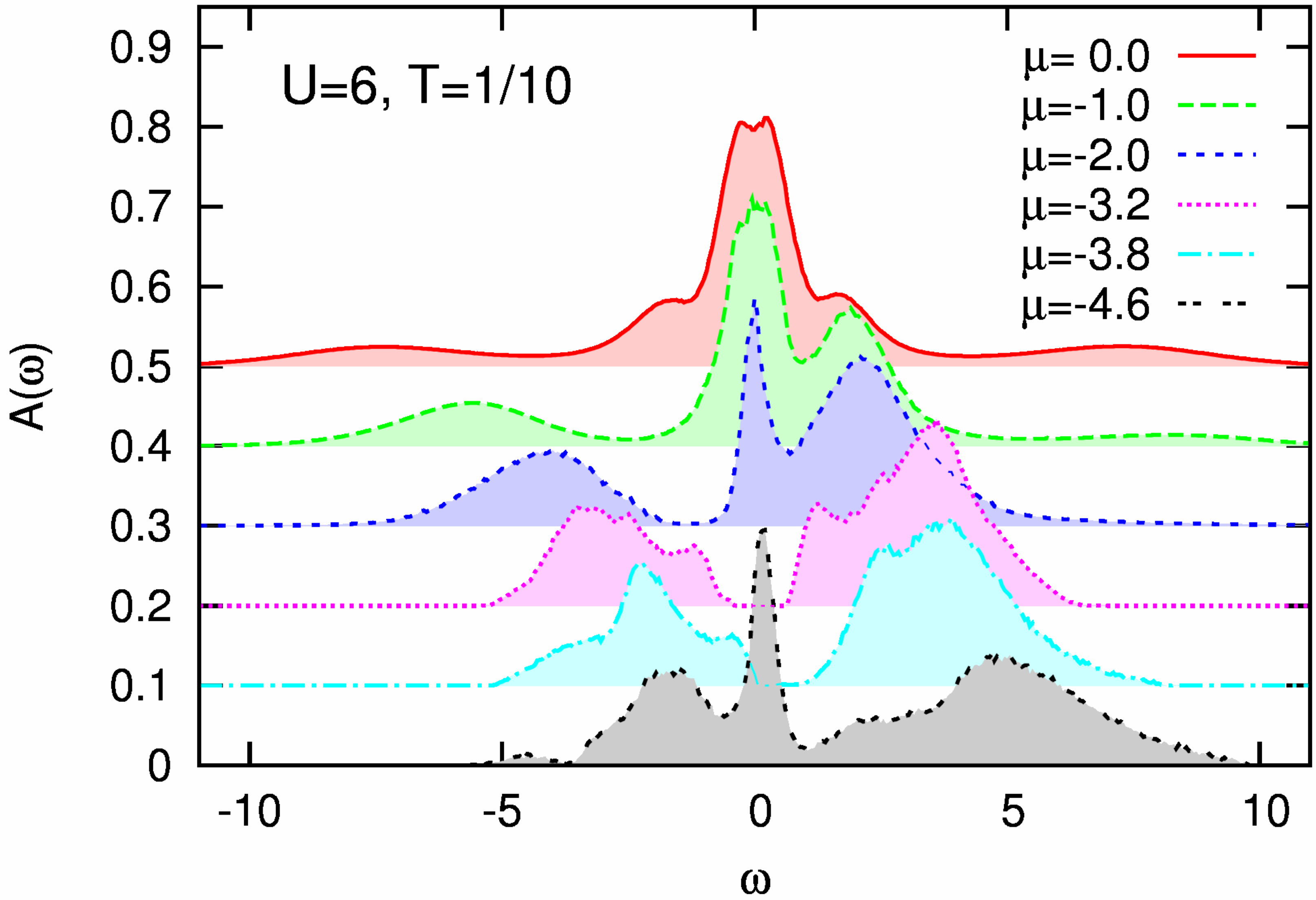

RAPID COMMUNICATIONS

PHYSICAL REVIEW A **80**, 051602(R) (2009)

Mott transitions in ternary flavor mixtures of ultracold fermions on optical lattices

E. V. Gorelik and N. Blümer
Institute of Physics, Johannes Gutenberg University, 55099 Mainz, Germany
(Received 7 May 2009; revised manuscript received 9 July 2009; published 11 November 2009)

RAPID COMMUNICATIONS

PHYSICAL REVIEW A **81**, 021603(R) (2010)

Three-component fermionic atoms with repulsive interaction in optical lattices

Shin-ya Miyatake,[1] Kensuke Inaba,[2] and Sei-ichiro Suga[1,3]
[1]*Department of Applied Physics, Osaka University, Suita, Osaka 565-0871, Japan*
[2]*NTT Basic Research Laboratories, NTT Corporation, Atsugi 243-0198, Japan, and CREST, JST, Chiyoda-ku, Tokyo 102-0075, Japan*
[3]*Department of Materials Science and Chemistry, University of Hyogo, Himeji 671-2280, Japan*
(Received 4 December 2009; published 17 February 2010)

- MIT at integer filling (same authors, Physica C)
- inequivalent flavors
- ordering at half filling

Antiferromagnetic order at finite T in an optical trap

Now include trapping potential, e.g.: $V_i = V r_i^2$

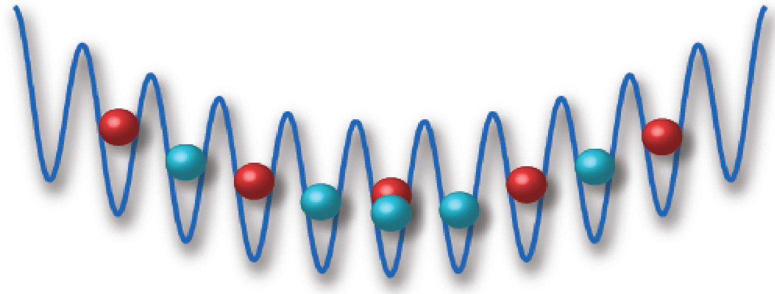

$$H = -\sum_{(ij),\sigma} t_{ij}\, c^\dagger_{i\sigma} c_{j\sigma} + U \sum_{i=1}^{N} n_{i\uparrow} n_{i\downarrow} + \sum_{i,\sigma} V_i\, n_{i\sigma}$$

Antiferromagnetic order at finite T in an optical trap

Now include trapping potential, e.g.: $V_i = V r_i^2$

$$H = -\sum_{(ij),\sigma} t_{ij}\, c^\dagger_{i\sigma} c_{j\sigma} + U \sum_{i=1}^{N} n_{i\uparrow} n_{i\downarrow} + \sum_{i,\sigma} V_i\, n_{i\sigma}$$

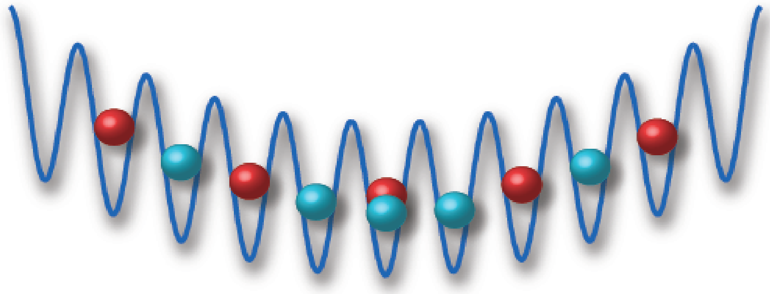

Real-space DMFT: use local self-energy in inhomogeneous system

$\rightsquigarrow$ N single-site impurities, coupled by modified lattice Dyson equation:

$$\left[G_\sigma(i\omega_n)\right]^{-1}_{ij} = \left(\mu_\sigma + i\omega_n\right)\delta_{ij} - t_{ij} - \left(V_i + \Sigma_{i\sigma}(i\omega_n)\right)\delta_{ij}$$

[M. Snoek, I. Titvinidze, C. Toke, K. Byczuk, and W. Hofstetter, New Journal of Physics (2008); R. Helmes, T. A. Costi, and A. Rosch, PRL (2008)]

Also: inhomogeneous DMFT (for Falicov-Kimball model) [Freericks]

Antiferromagnetic order at finite T in an optical trap

Now include trapping potential, e.g.: $V_i = V r_i^2$

$$H = -\sum_{(ij),\sigma} t_{ij}\, c^\dagger_{i\sigma} c_{j\sigma} + U \sum_{i=1}^{N} n_{i\uparrow} n_{i\downarrow} + \sum_{i,\sigma} V_i\, n_{i\sigma}$$

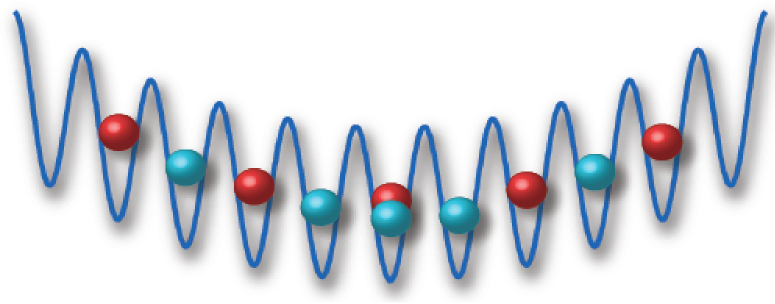

Real-space DMFT: use local self-energy in inhomogeneous system

$\rightsquigarrow$ N single-site impurities, coupled by modified lattice Dyson equation:

$$\left[G_\sigma(i\omega_n)\right]^{-1}_{ij} = \left(\mu_\sigma + i\omega_n\right)\delta_{ij} - t_{ij} - \left(V_i + \Sigma_{i\sigma}(i\omega_n)\right)\delta_{ij}$$

[M. Snoek, I. Titvinidze, C. Toke, K. Byczuk, and W. Hofstetter, New Journal of Physics (2008); R. Helmes, T. A. Costi, and A. Rosch, PRL (2008)]

Also: inhomogeneous DMFT (for Falicov-Kimball model) [Freericks]

Note: impurity problem is site-parallel, lattice Dyson equation is frequency-parallel

All previous implementations: RDMFT+NRG

RDMFT-NRG results in 2 dimensions

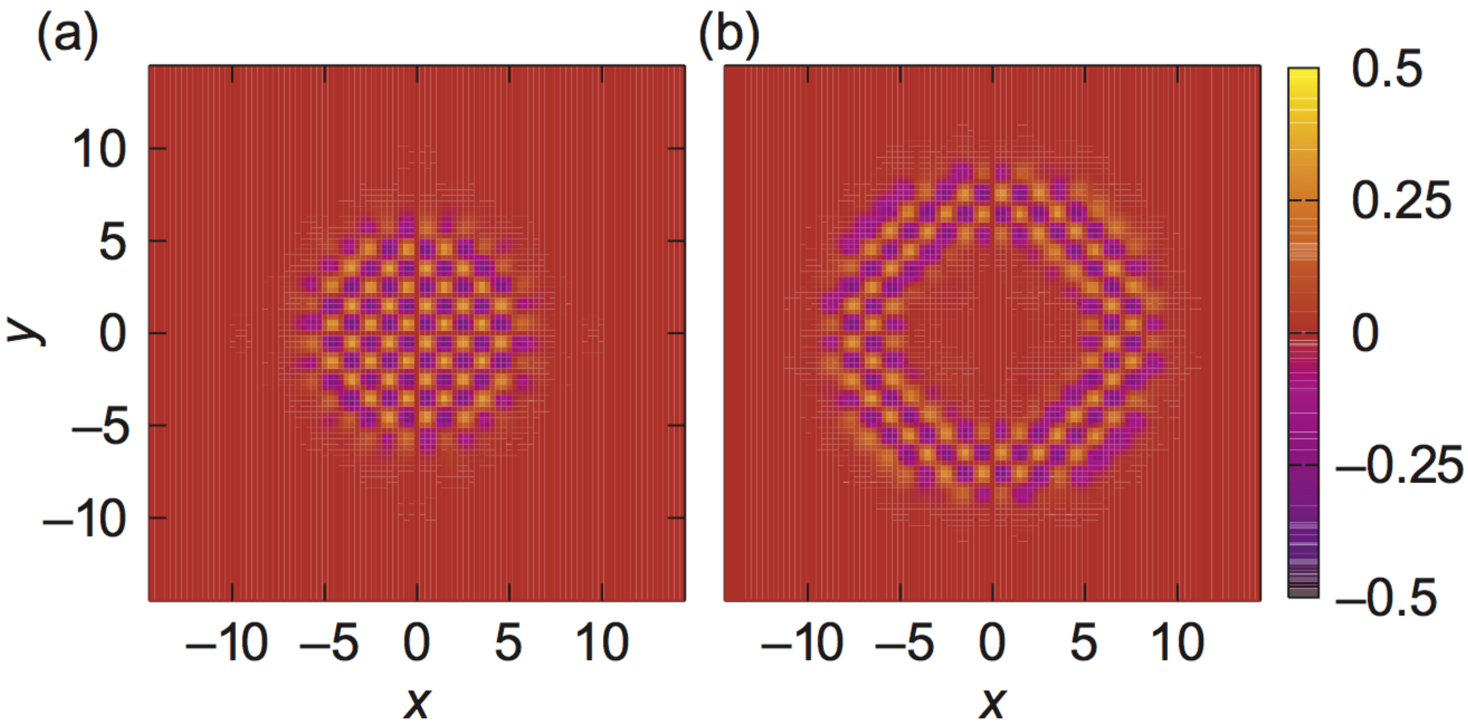

Figure 1. Real-space magnetization profiles for $U = 10$ on a square (30×30) lattice; (a) $V = 0.1$ and $\mu_\uparrow = \mu_\downarrow = 5$; (b) $V = 0.2$ and $\mu_\uparrow = \mu_\downarrow = 15$. Energies are expressed in units of the hopping parameter J.

[Snoek, Titvinidze, Töke, Byczuk, Hofstetter, NJP **10**, 093008 (2008)]

RDMFT-NRG results in 2 dimensions

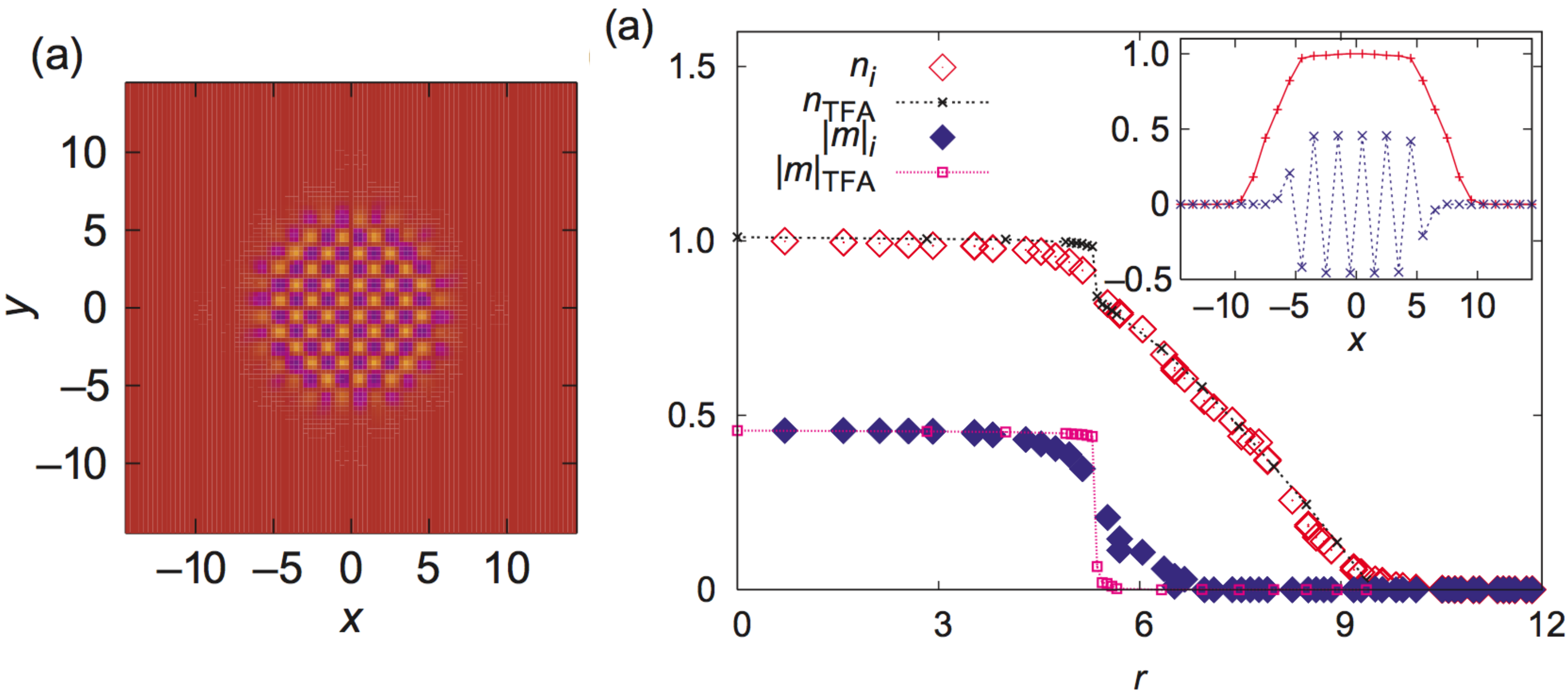

Figure 1. Real-space magnetization profiles for $U = 10$ on a square (30×30) lattice; (a) $V = 0.1$ and $\mu_\uparrow = \mu_\downarrow = 5$; (b) $V = 0.2$ and $\mu_\uparrow = \mu_\downarrow = 15$. Energies are expressed in units of the hopping parameter J.

[Snoek, Titvinidze, Töke, Byczuk, Hofstetter, NJP **10**, 093008 (2008)]

But: NRG problematic at elevated temperatures

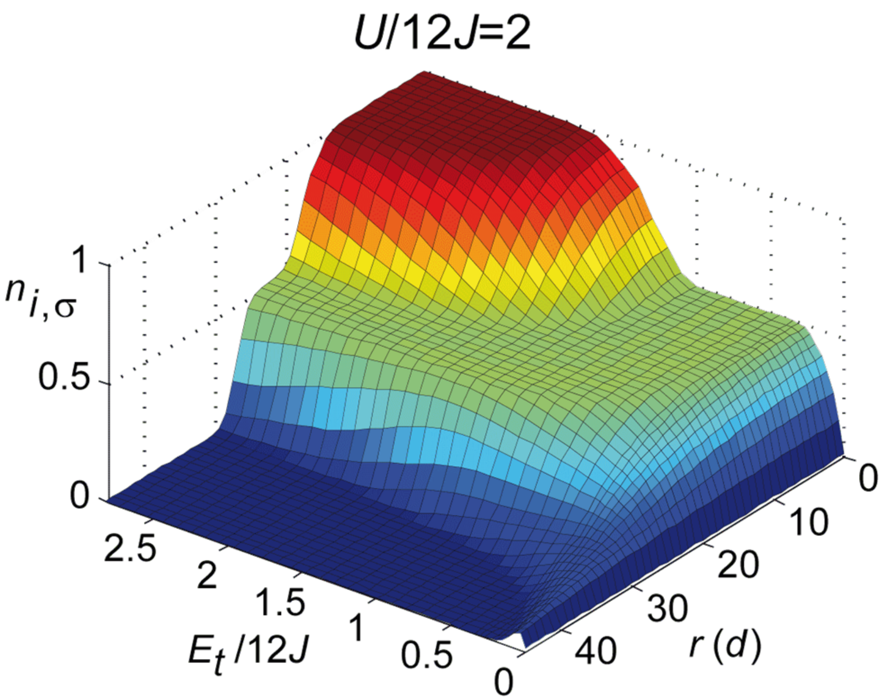

$T = 0.07t$

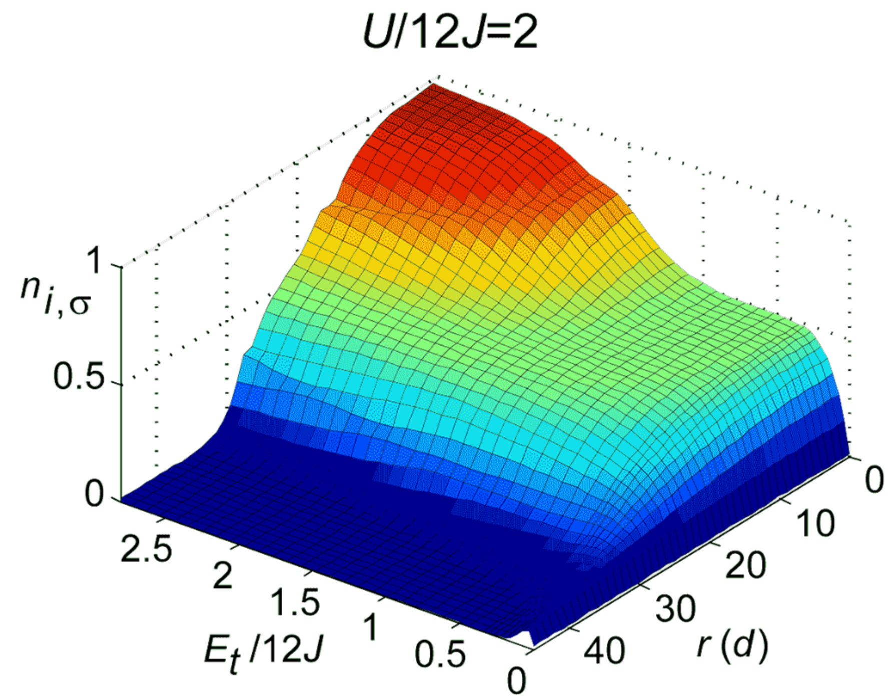

$T = 0.15t$

Additional plateau/kinks at $n_\sigma \approx 0.8$ for $T = 0.15t$ [Rosch group, courtesy of U. Schneider]

However: experimental temperatures are high $\rightsquigarrow$ advantage for QMC!

Real-space DMFT results for paramagnetic phase: QMC vs. NRG

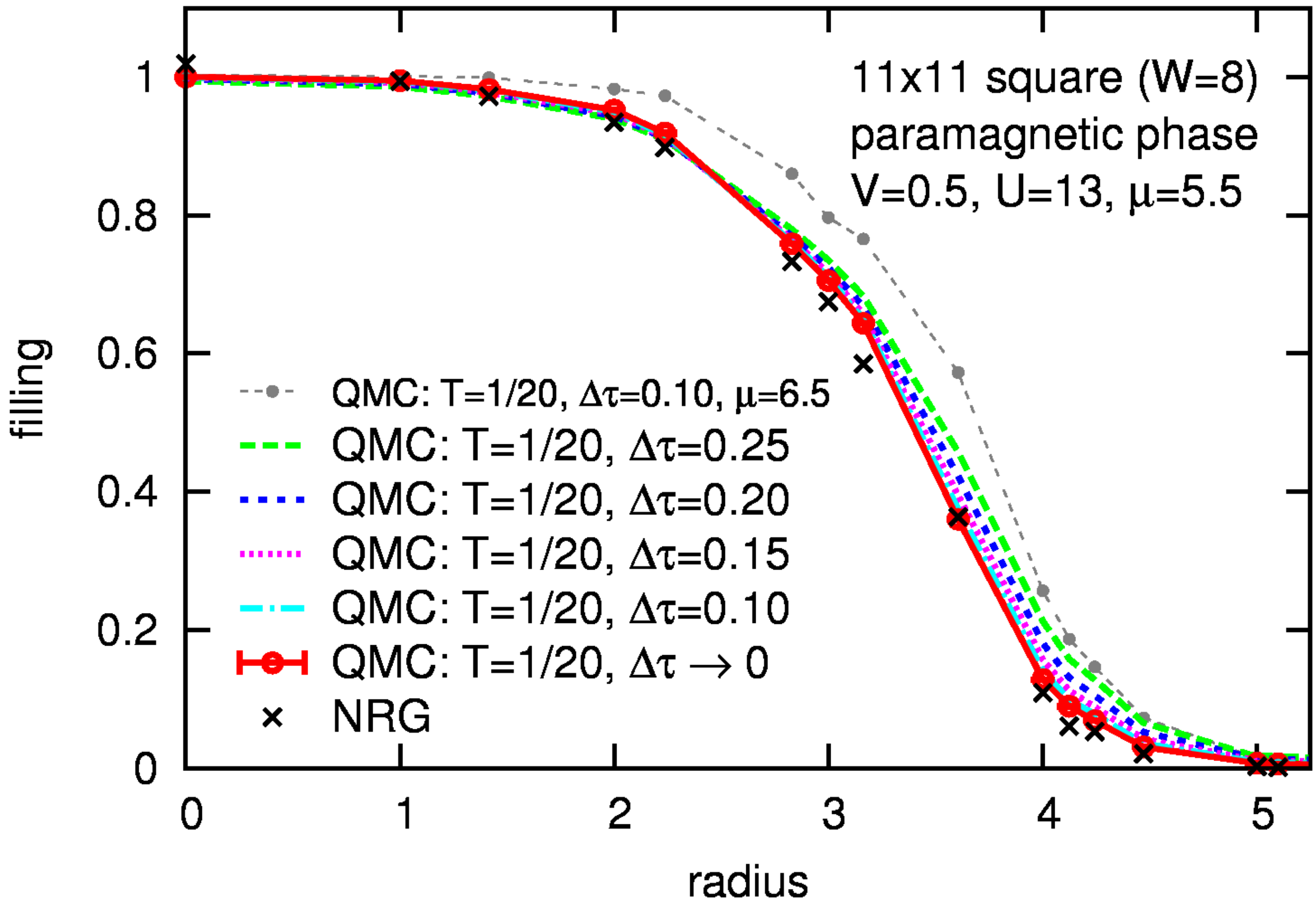

Good agreement QMC ↔ NRG (at low/zero T)   not shown: NRG worse for AF

[NRG data by I. Titvinidze (collaboration within SFB/TR 49)]

Melting of a central antiferromagnetic phase

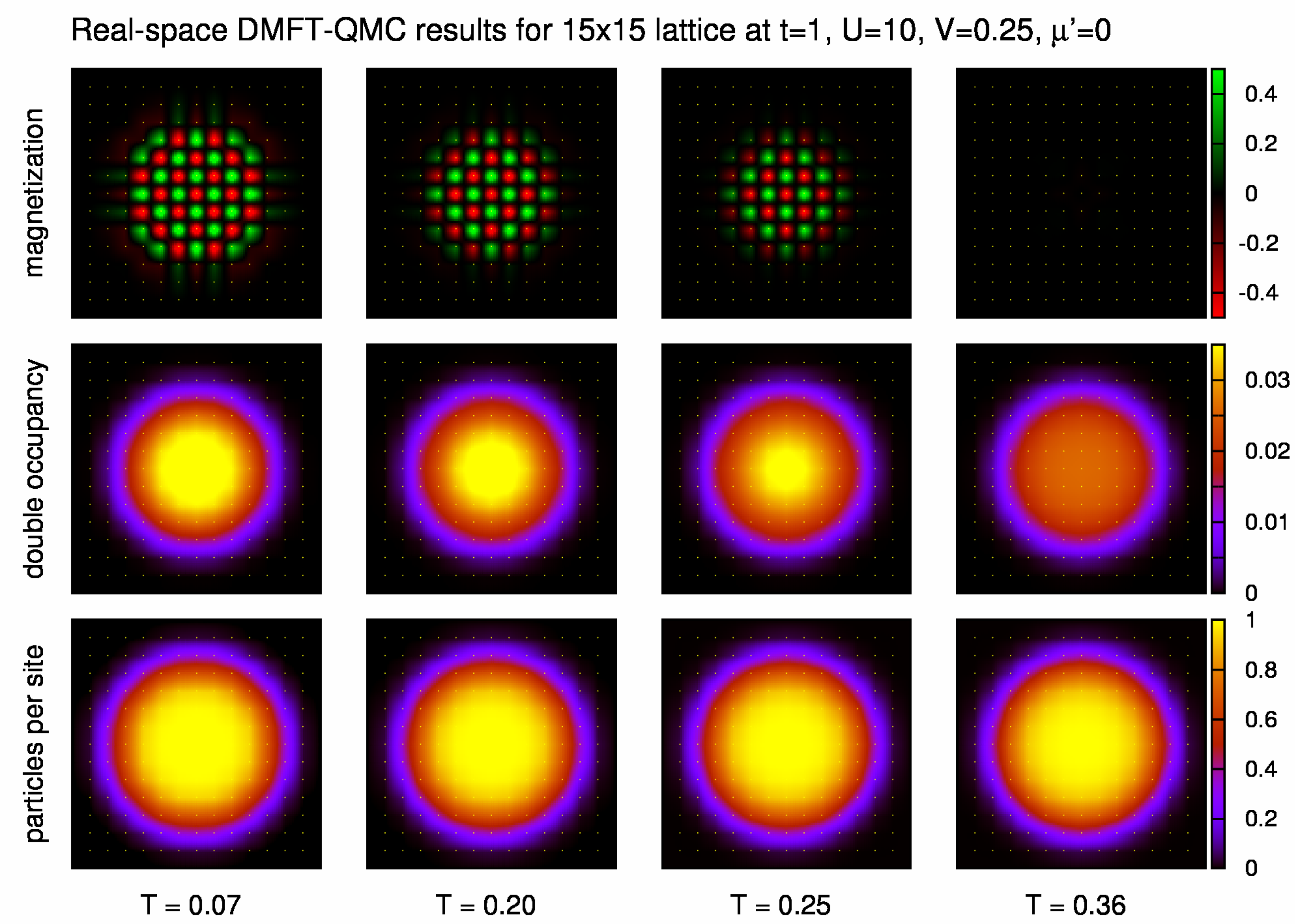

Antiferromagnetic order signaled by enhanced double occupancy - entropy?

Entropy: no direct computation, but from relations such as $dS/d\mu = dN/dT$

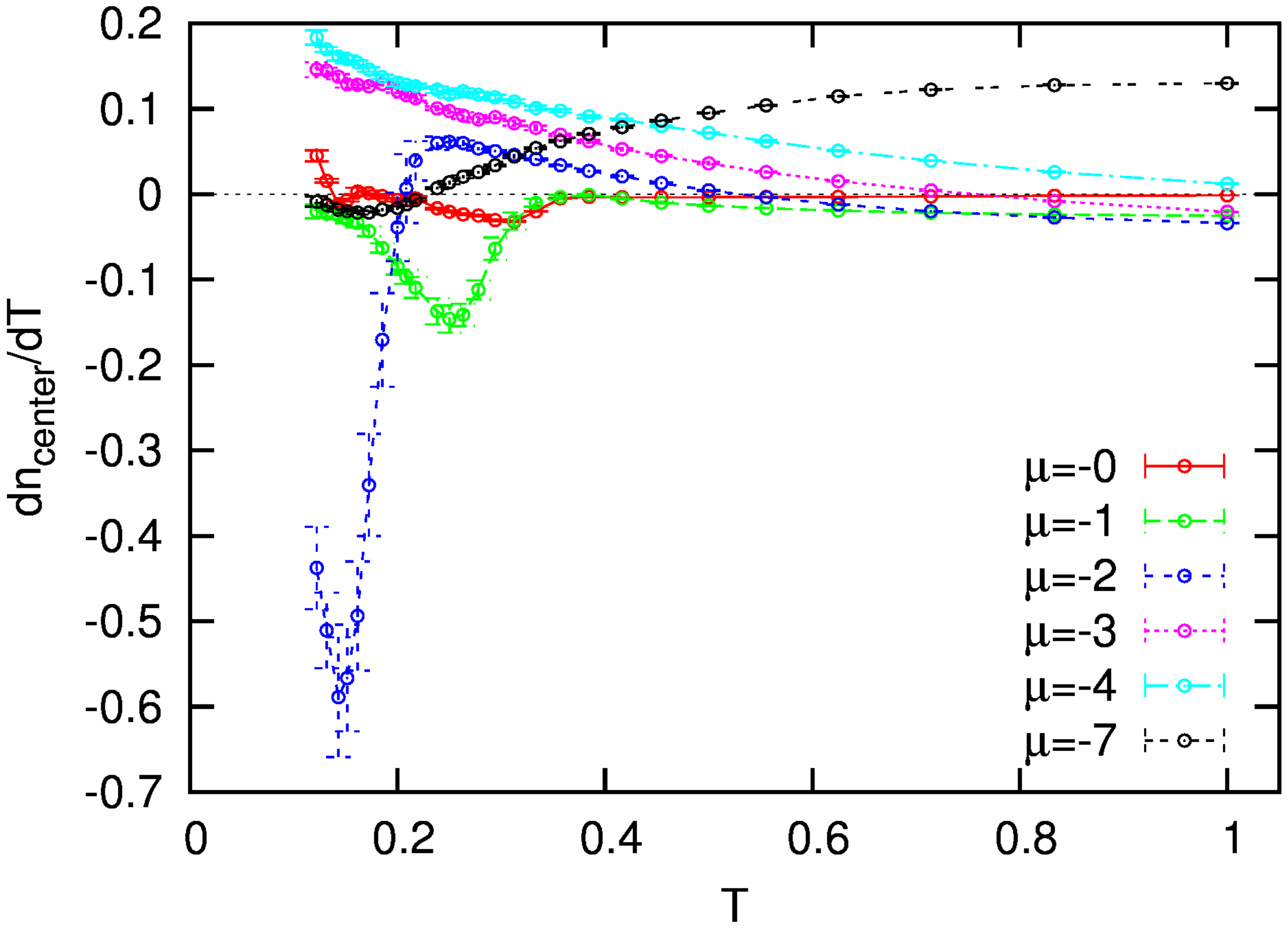

Example: derivative of central density (at $U = 10$, $V = 0.25$) for various μ

Strong negative peak at Neel temperature ($\rightsquigarrow$ need fine integration grid)

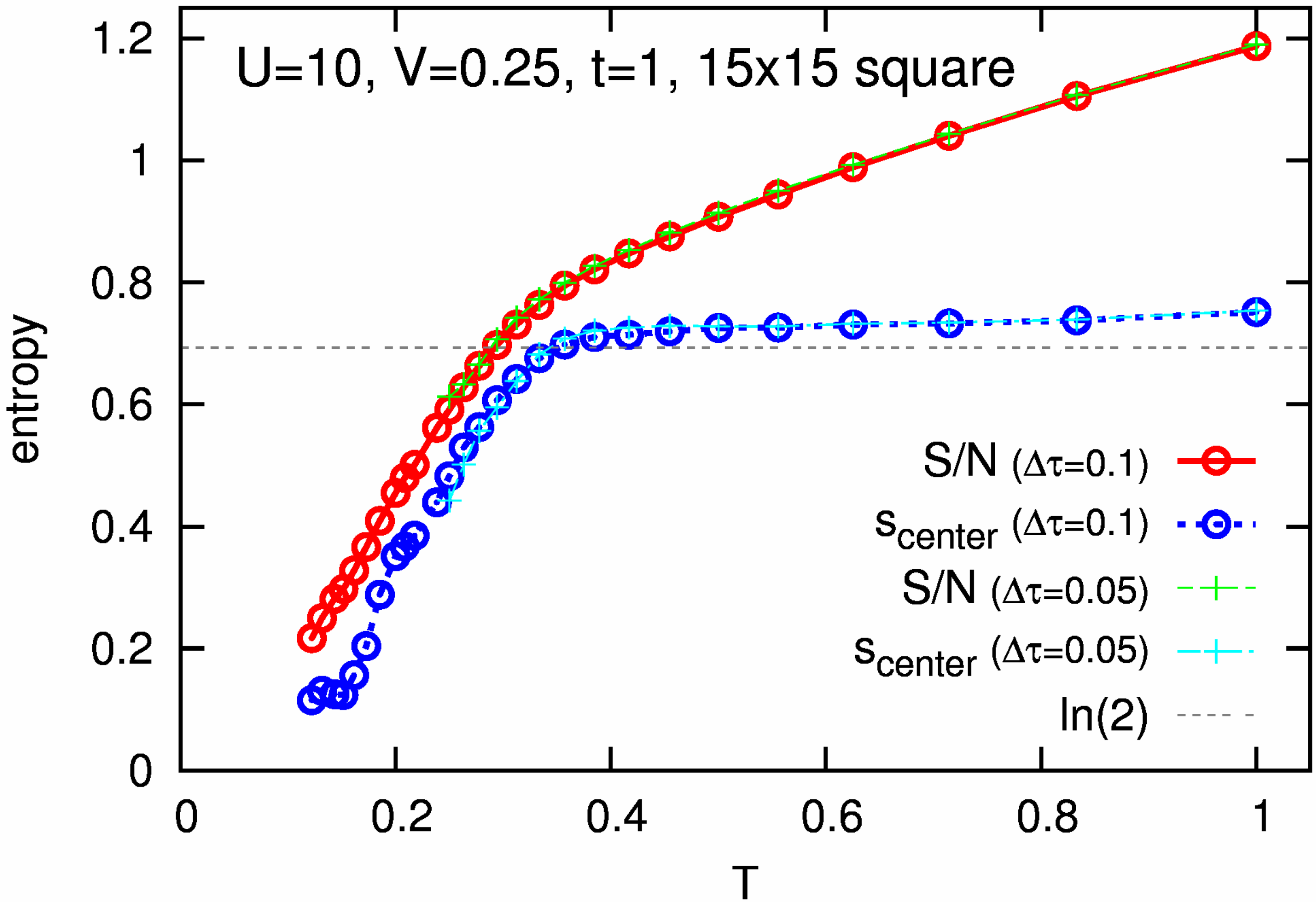

very small discretization dependence

Important: central entropy can be much smaller than average entropy!

Simulations of 3D systems with $\mathcal{O}(10^5)$ particles

Naive full RDMFT simulation of experimental situation requires $M = 100^3$ lattice

Scaling: QMC CPU time $\propto M$

Green function memory $\propto M^2$

Green function inversion time $\propto M^3$

Simulations of 3D systems with $\mathcal{O}(10^5)$ particles

Naive full RDMFT simulation of experimental situation requires $M = 100^3$ lattice

Scaling: QMC CPU time $\propto M$

Green function memory $\propto M^2$

Green function inversion time $\propto M^3$

Practical (dense inversion, fully parallel): $\lesssim$ 10000 sites $\rightsquigarrow$ need smart strategies

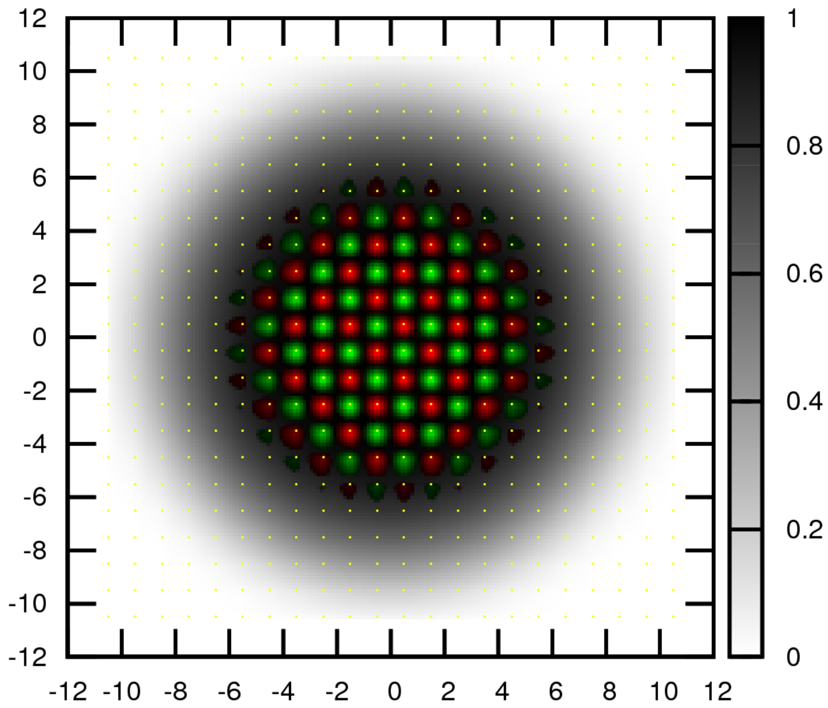

Simulations of 3D systems with $\mathcal{O}(10^5)$ particles

Naive full RDMFT simulation of experimental situation requires $M = 100^3$ lattice

Scaling: QMC CPU time $\propto M$

Green function memory $\propto M^2$

Green function inversion time $\propto M^3$

Practical (dense inversion, fully parallel): $\lesssim$ 10000 sites $\rightsquigarrow$ need smart strategies

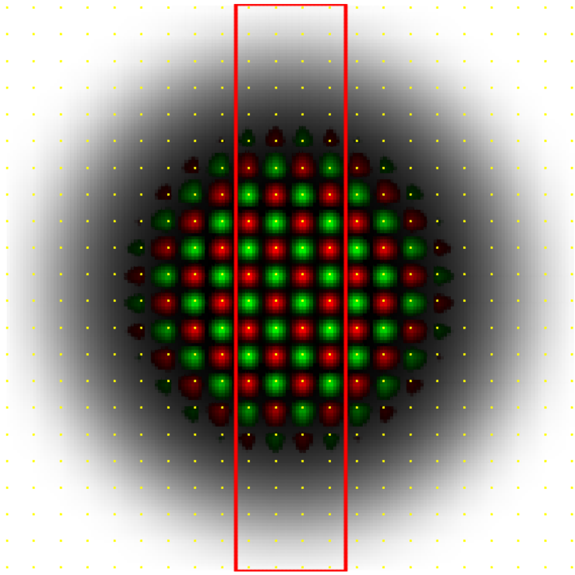

Simulations of 3D systems with $\mathcal{O}(10^5)$ particles

Naive full RDMFT simulation of experimental situation requires $M = 100^3$ lattice

Scaling: QMC CPU time $\propto M$

Green function memory $\propto M^2$

Green function inversion time $\propto M^3$

Practical (dense inversion, fully parallel): $\lesssim$ 10000 sites $\rightsquigarrow$ need smart strategies

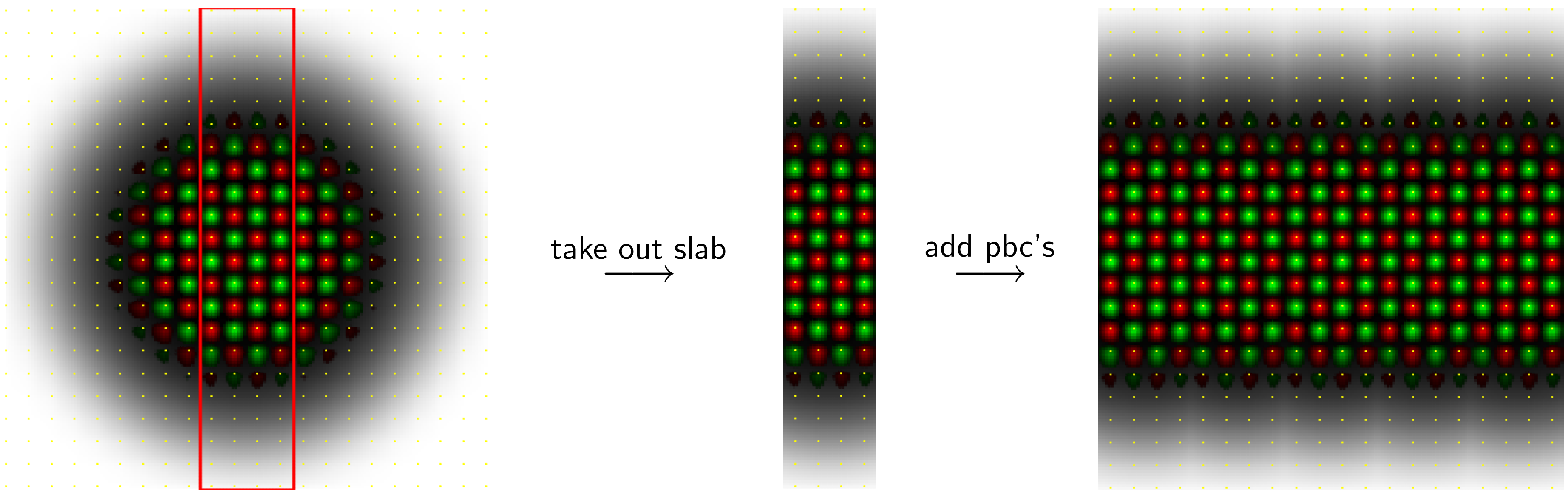

In practice: cylindrical potential (equivalent layers)

Alternative: 3D calculation, but focus on AF core (pbc's in all 3 directions):

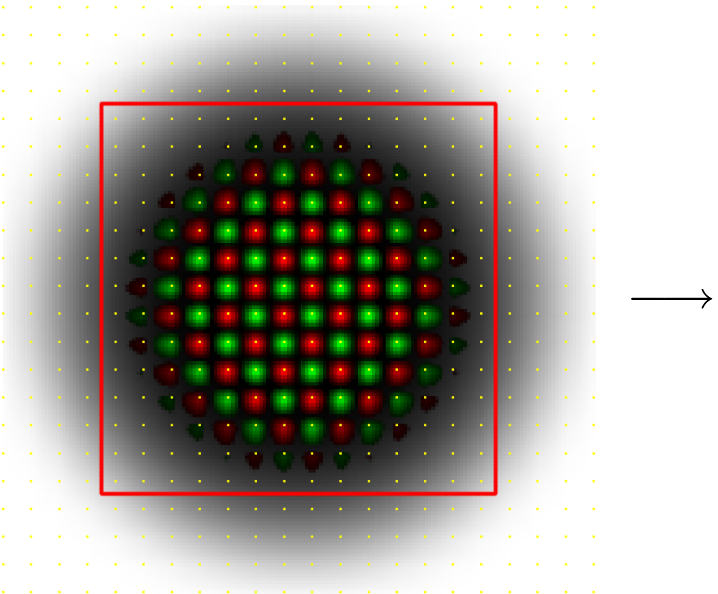

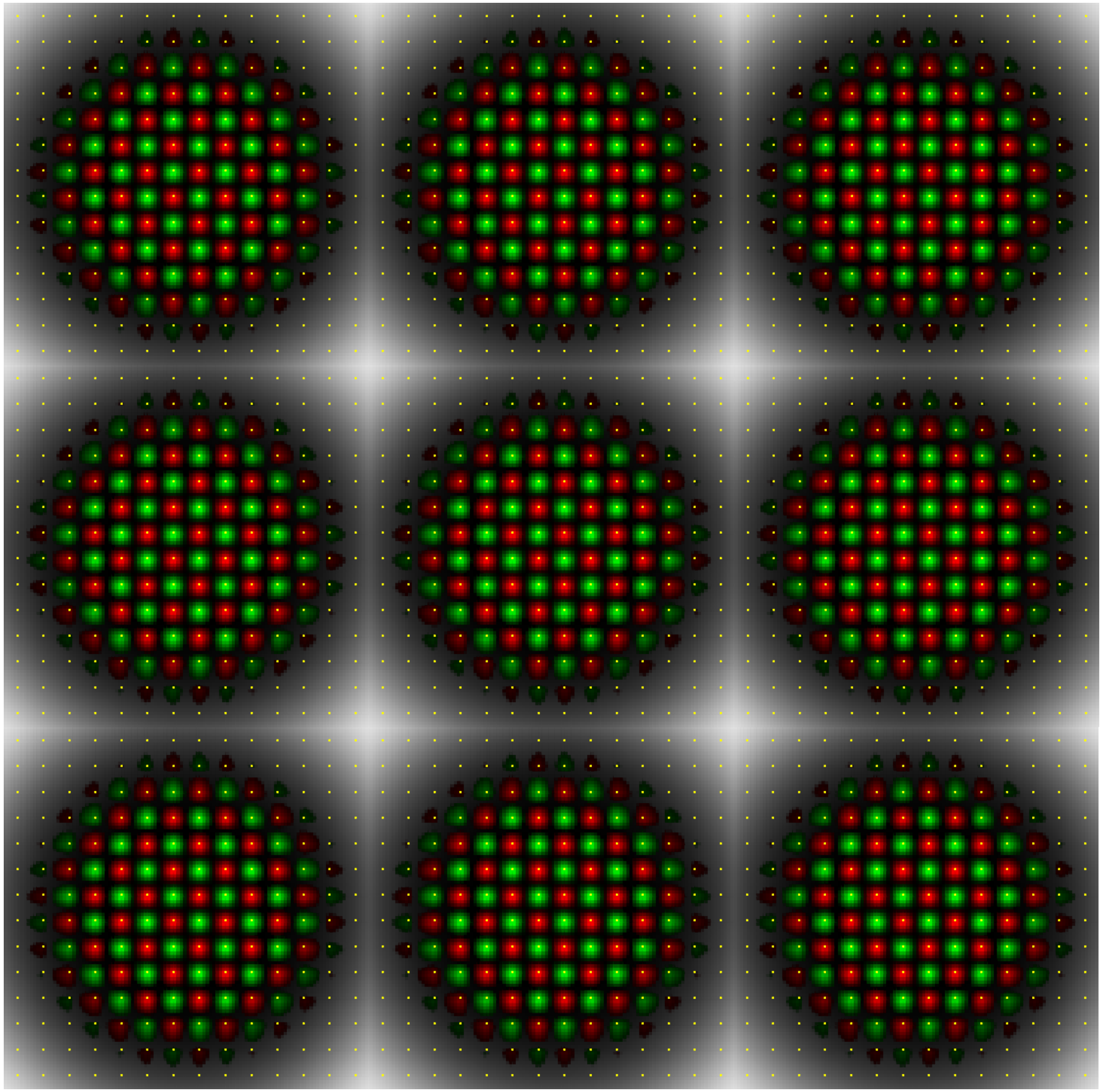

Most efficient: slab calculation focussing on AF core (with pbc)

Test: slab versus minimal core 3D calculation (all with pbc)

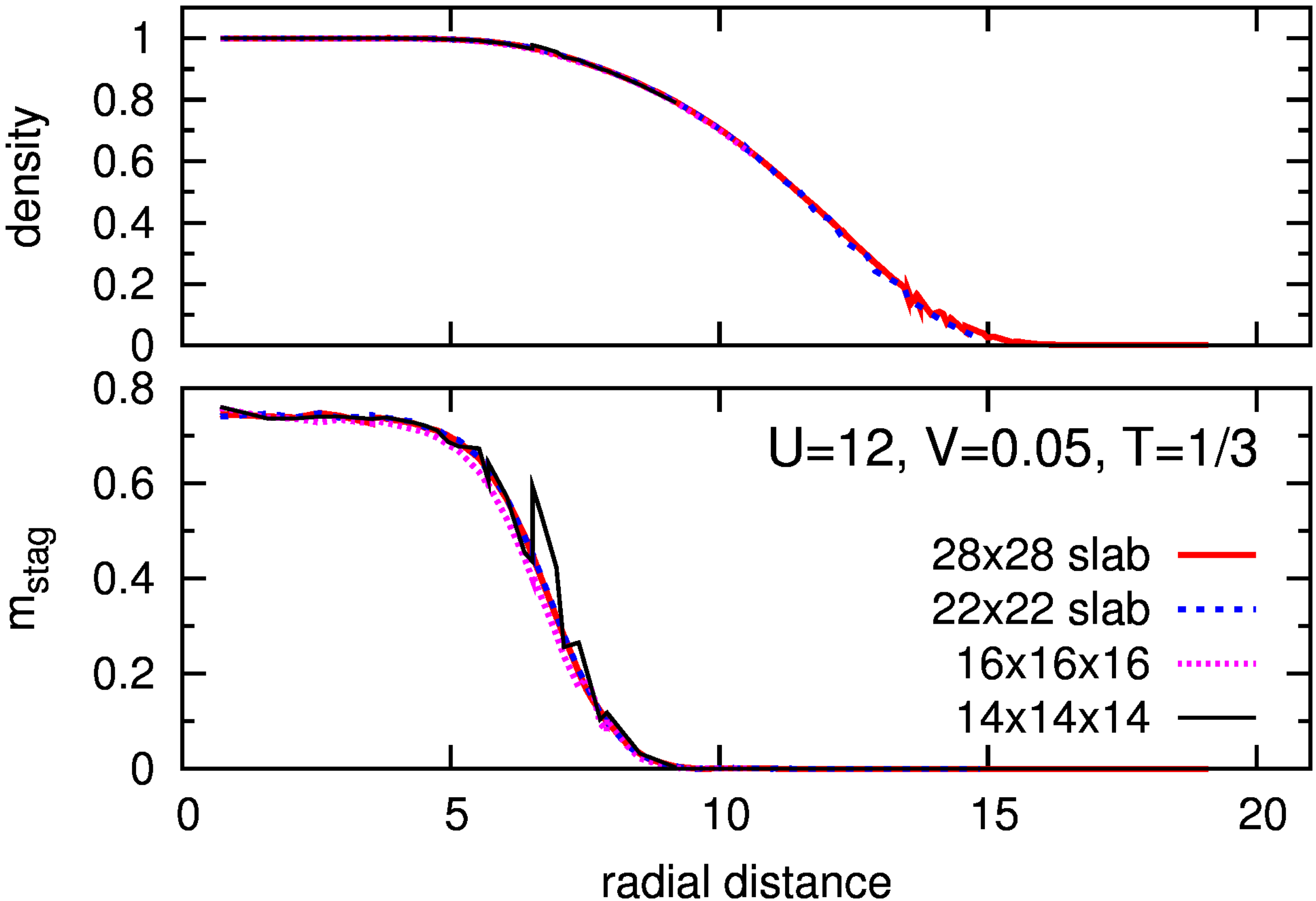

Significant deviations only if core touches boundaries!

RDMFT-QMC results (cubic lattice, $V = 0.05t$, $U = W = 12t$)

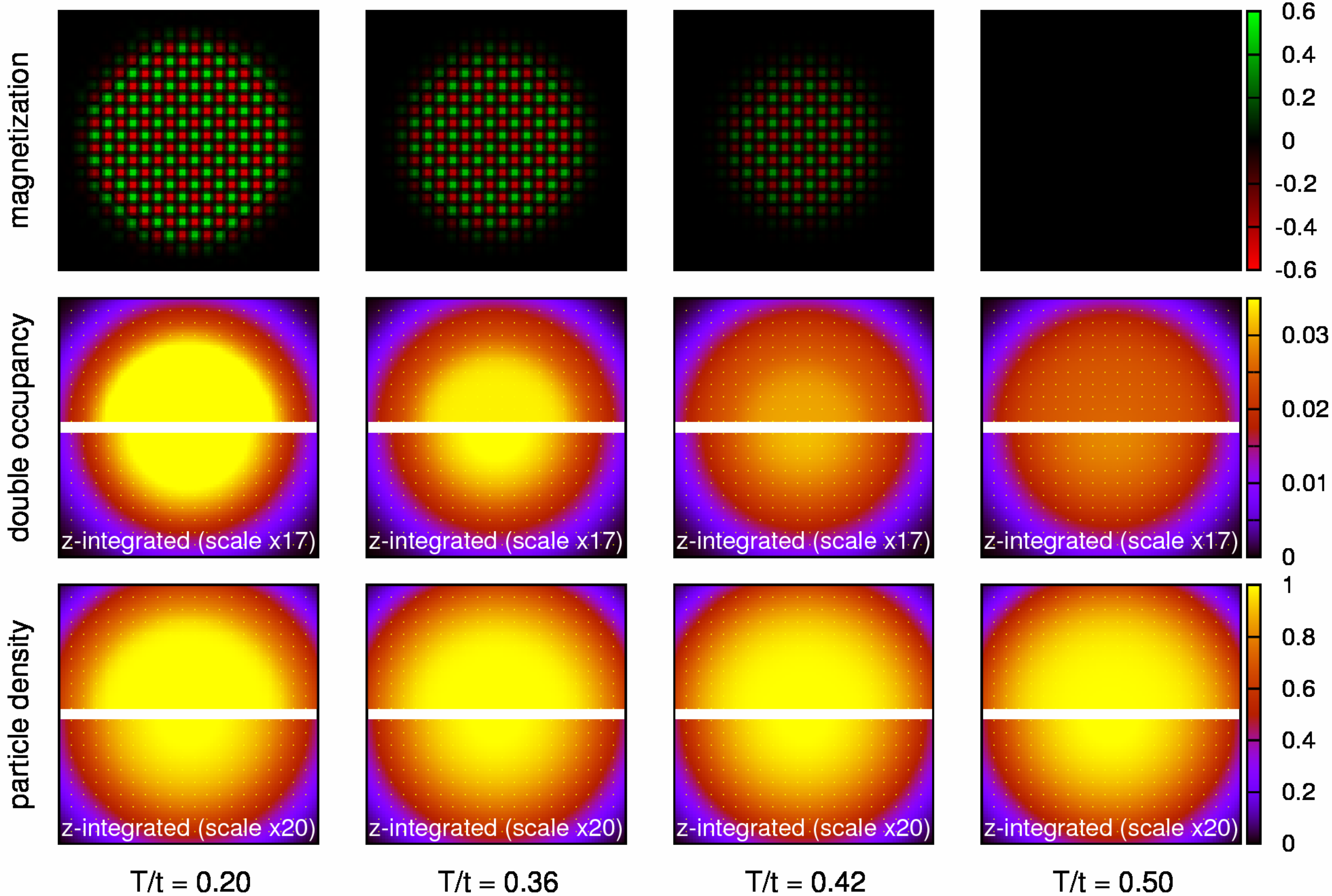

RDMFT-QMC results (cubic lattice, $V = 0.05t$, $U = W = 12t$)

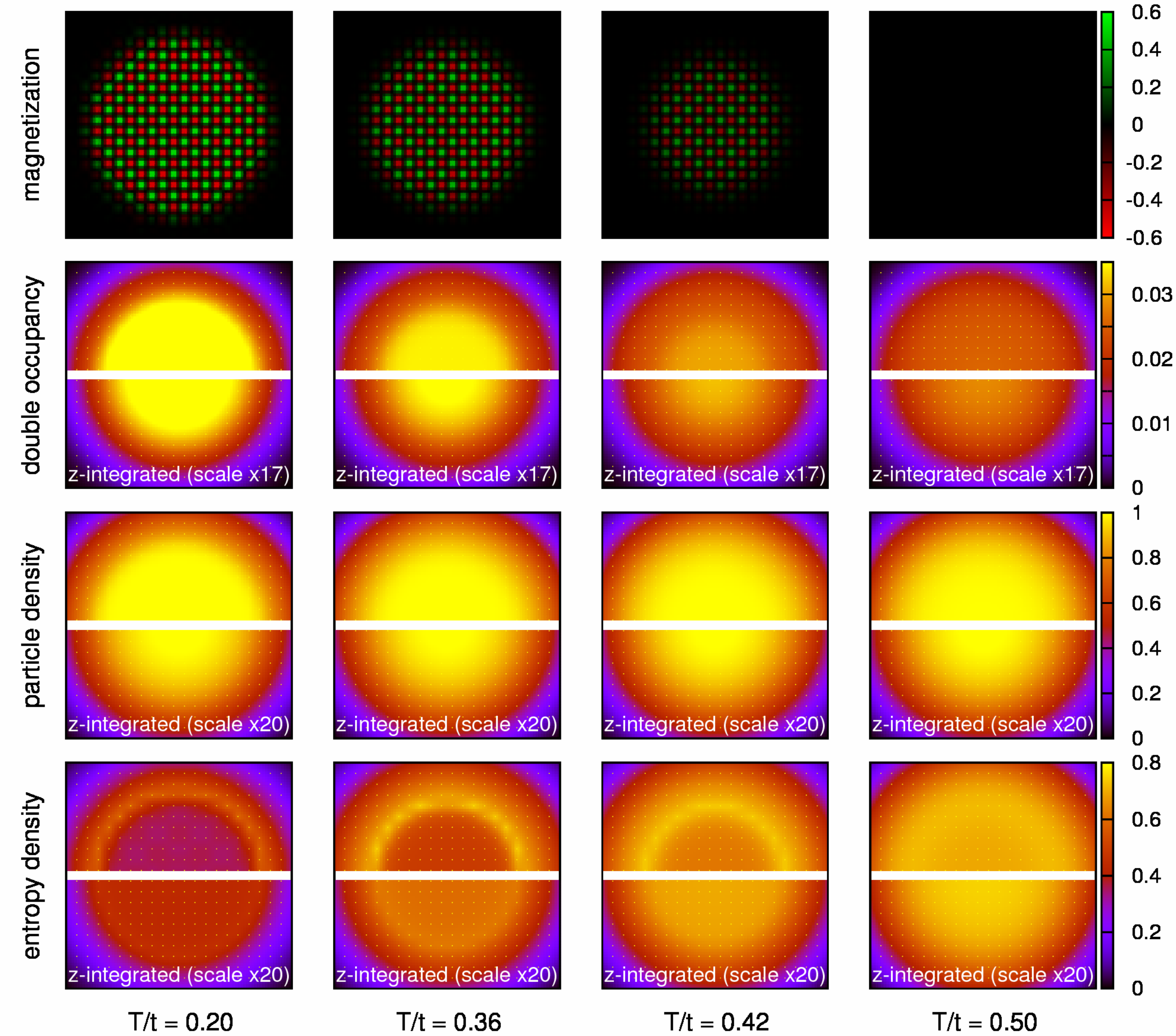

AF core:

nearly fully polarized at $T = 0.20t$

vanishes at $T_N \approx 0.46t$

AF $\leftrightarrow$ enhanced D!

$\sim$ 6000 atoms (naively $\sim 30^3 = 27000$ sites needed)

Entropy

$$S = \int_{-\infty}^{0} d\mu' \, \frac{dN}{dT}$$

Enhanced double occupancy: a signature of AF order

Illustration of mechanism for enhanced double occupancy (at strong coupling):

(a)

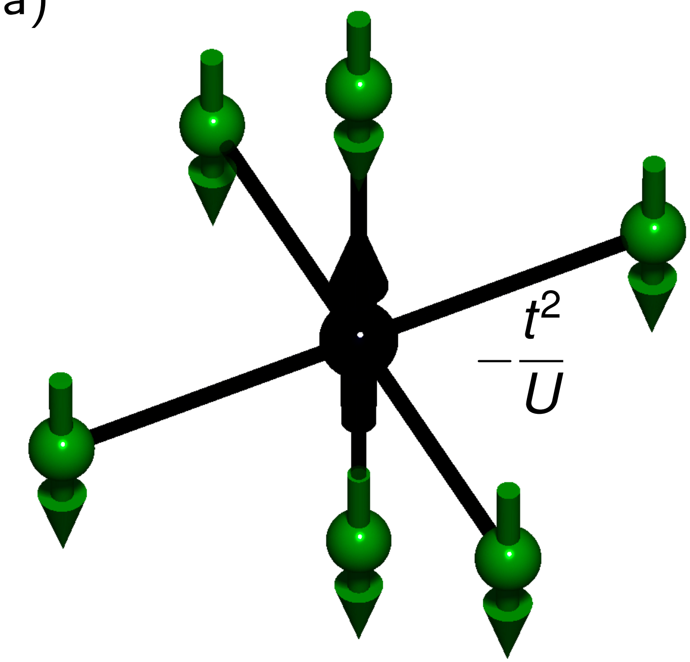

(b)

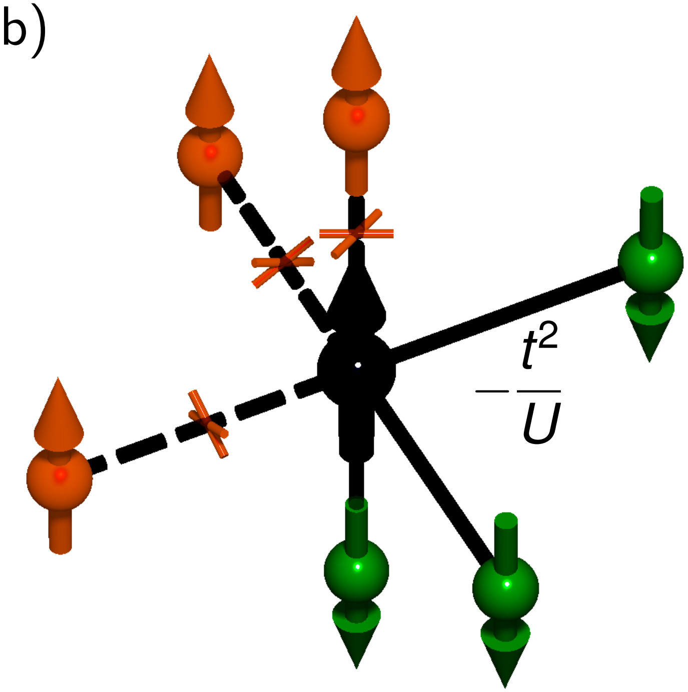

AF state:

electron can hop to all
$Z = 6$ next neighbors

$$E_{AF} = -\frac{Z\,t^2}{U}$$

Paramagnetic state:

1/2 of the neighboring sites
are forbidden for hopping

$$E_p = -\frac{Z\,t^2}{2U}$$

By $D = dE/dU$ (at $T = 0$), the argument implies $D_{\mathbf{AF}}/D_{\mathbf{p}} \xrightarrow{U\to\infty} 2$.

DMFT-QMC estimates of D at half filling

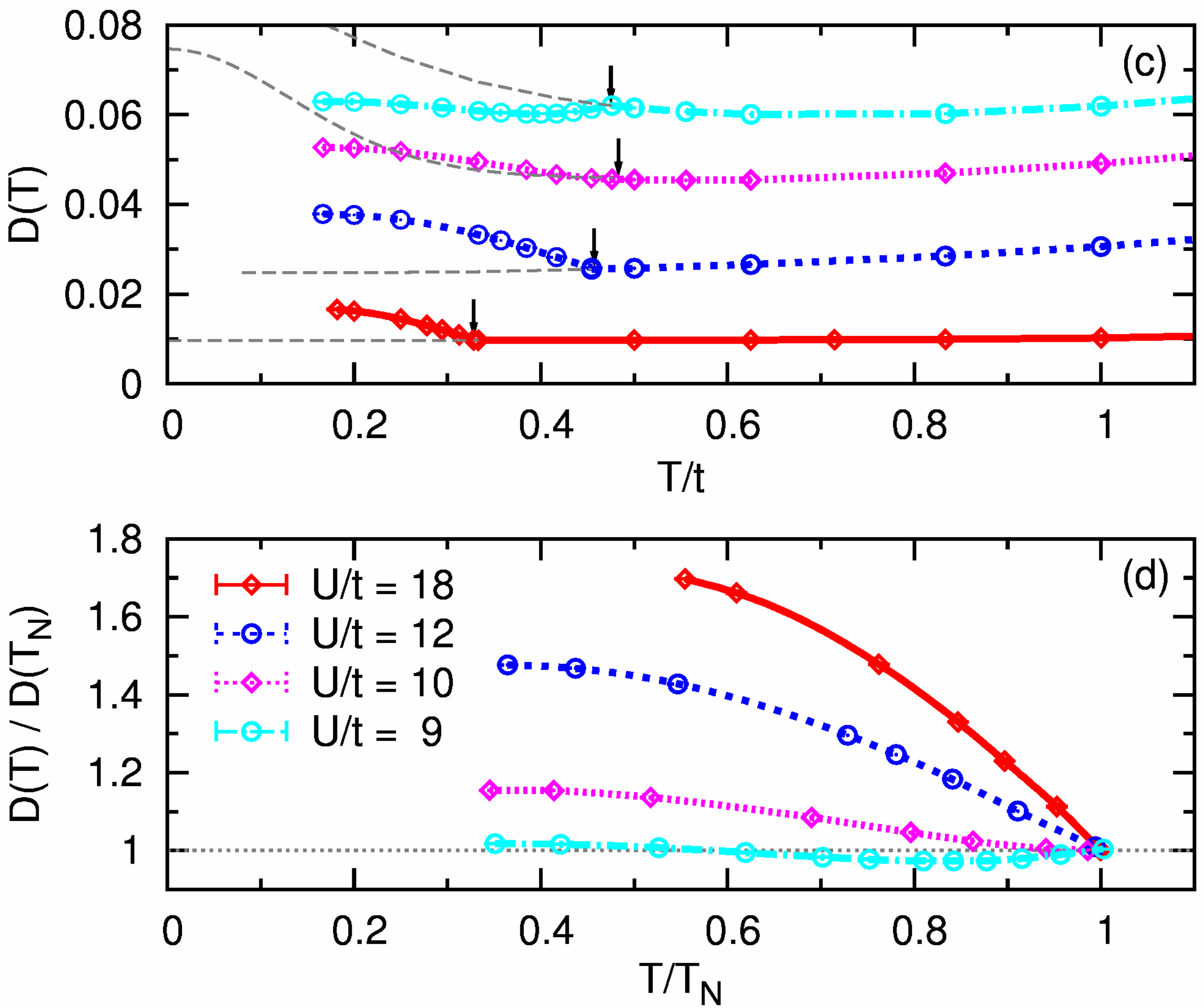

AF $\Rightarrow$
enhanced D at $U \gtrsim 10t$

arrows: Néel temperatures

thin lines: metastable paramagnetic phase.

Data scaled to values of critical point:

relative enhancement
$D/D(T_\mathrm{N}) \stackrel{U\to\infty}{\longrightarrow} 2$

Note: AF kills Pomeranchuk cooling [Werner, Parcollet, Georges, Hassan, PRL (2005)]!

Radial dependence of m_{stag} and D: RDMFT calculations ($V = 0.05t$)

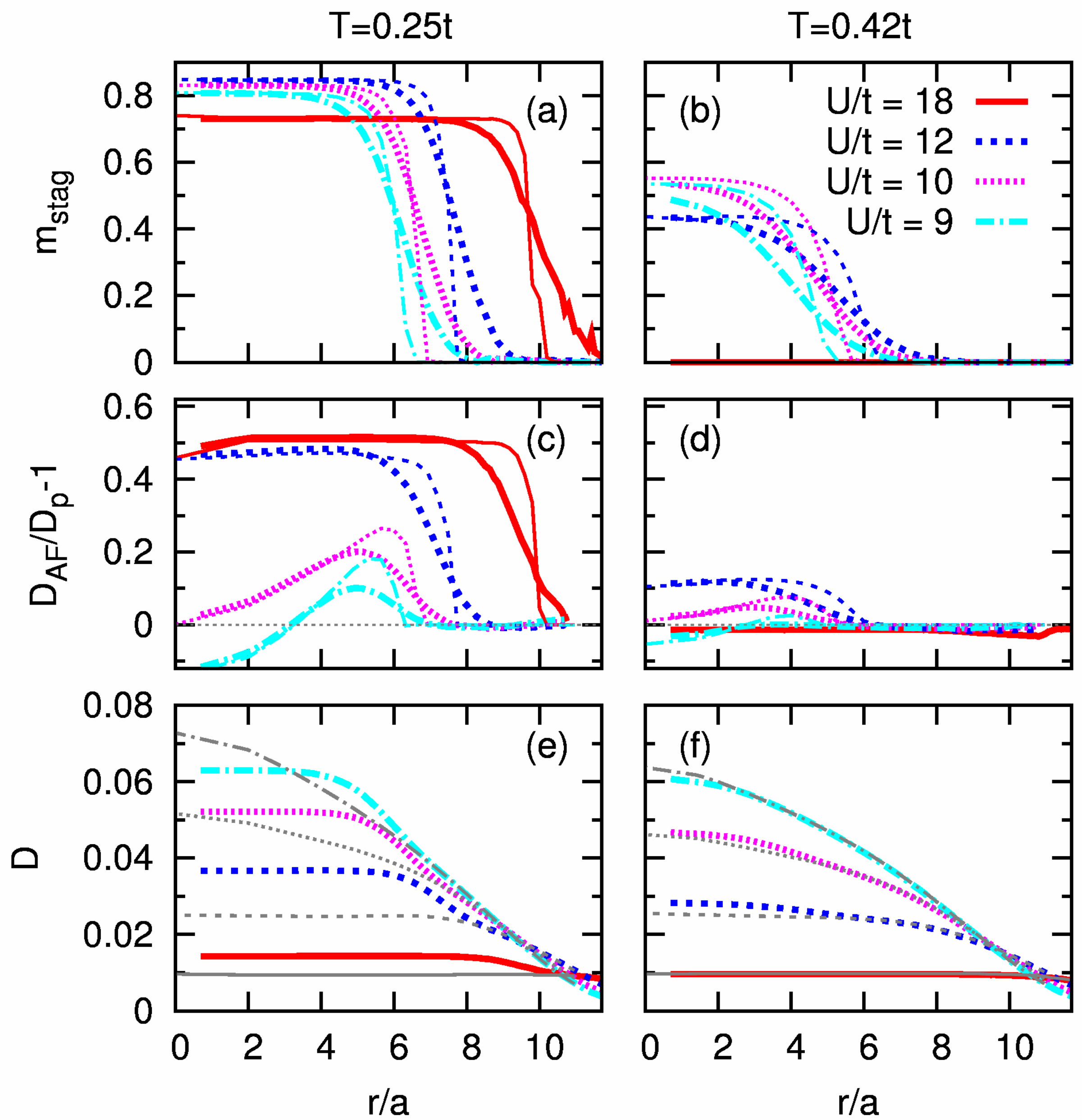

Strong proximity effects beyond LDA (thin lines in a-d)

Relative enhancement of D in the AF phase:

$\sim$ same for $U = 12t$ and $18t$ at fixed $T = 0.25t$

Néel transition visible in integrated quantities? Yes!

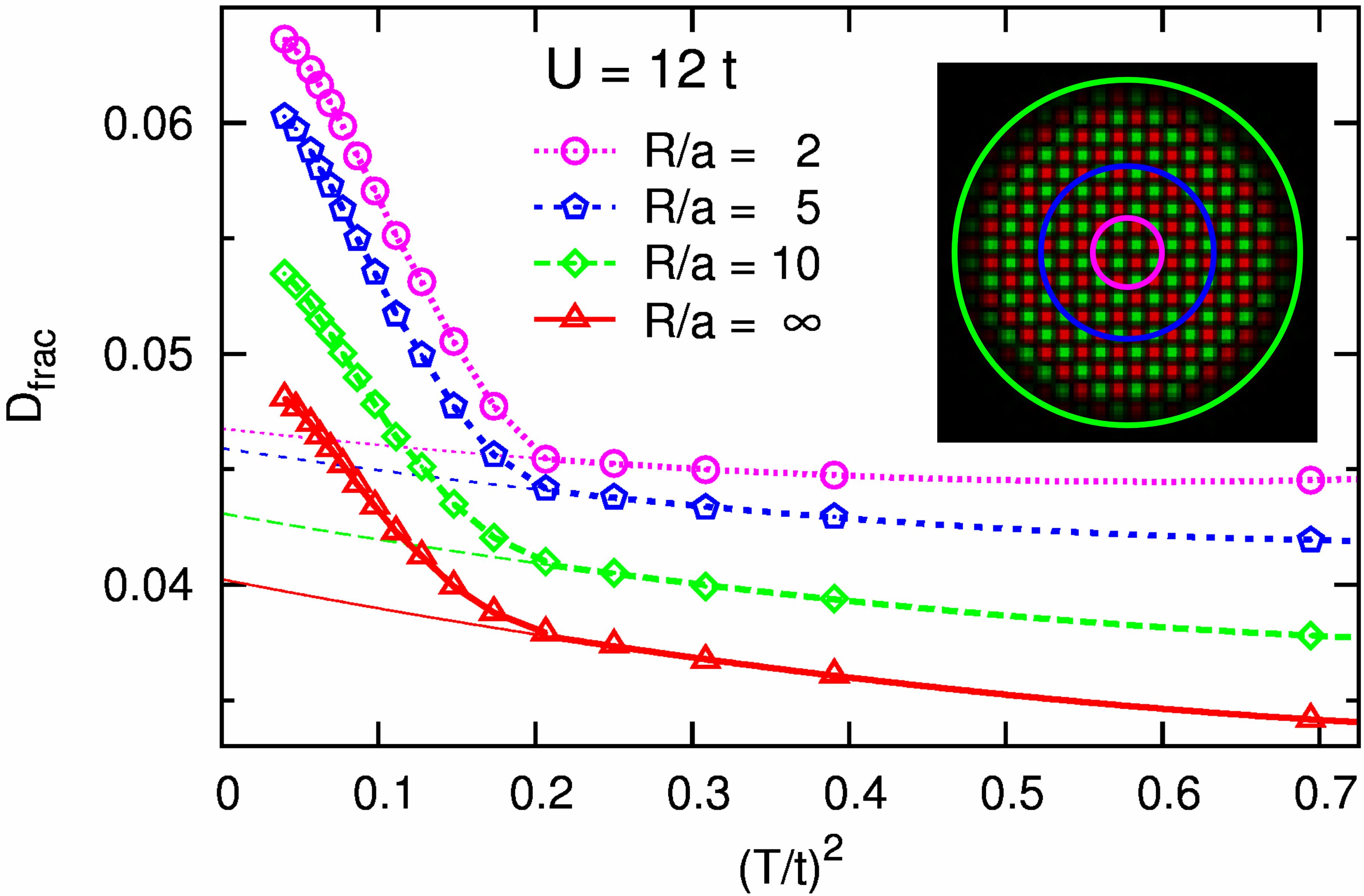

Summary

Multigrid HF-QMC method: numerically exact (quasi CT) + efficient

Mott transition for 3 degenerate flavors in (U, T, μ) space

Novel semi-compressible phase, spectra, small lattice effects

Real-space DMFT

Efficient and flexible RDMFT-QMC code

AF order at finite T signaled by enhanced D – LDA deficient

Summary

Multigrid HF-QMC method: numerically exact (quasi CT) + efficient

Mott transition for 3 degenerate flavors in (U, T, μ) space

Novel semi-compressible phase, spectra, small lattice effects

Real-space DMFT

Efficient and flexible RDMFT-QMC code

AF order at finite T signaled by enhanced D – LDA deficient

Outlook

3D calculations for realistic trap parameters and system sizes

Inequivalent spins/flavors: OSMT-like physics, ordered phases

Multigrid HF-QMC for RDMFT; impact of higher Bloch bands

Summary

Multigrid HF-QMC method: numerically exact (quasi CT) + efficient

Mott transition for 3 degenerate flavors in (U, T, μ) space

Novel semi-compressible phase, spectra, small lattice effects

Real-space DMFT

Efficient and flexible RDMFT-QMC code

AF order at finite T signaled by enhanced D – LDA deficient

Outlook

3D calculations for realistic trap parameters and system sizes

Inequivalent spins/flavors: OSMT-like physics, ordered phases

Multigrid HF-QMC for RDMFT; impact of higher Bloch bands

Spin-off: solids with large unit cells (distortions, surfaces, impurities, . . .)

Thanks to: Bloch, Esslinger, Hofstetter, van Dongen groups and DFG (TR49)